Design and Characterization of a Novel Filling Yarn Insertion System for Weaving Machines

by

Steven Brian Meeks

A thesis submitted to the Graduate Faculty of
Auburn University
in partial fulfillment of the
requirements for the Degree of
Master of Science

Auburn, Alabama
May 6, 2012

Approved by

Sabit Adanur, Chair, Professor of Polymer and Fiber Engineering
Peter Schwartz, Professor and Head of Polymer and Fiber Engineering
Michael Baginski, Associate Professor of Electrical Engineering
Dan Marghitu, Professor of Mechanical Engineering

Abstract

Weaving is a textile manufacturing process in which weft yarns are inserted by machines through a gap in the warp yarns called a shed to form a woven fabric through interlacing. The filling insertion systems that are currently being used in the market have reached their maximum potential in terms of speed and production rate. There are also limitations that the current methods face such as a finite maximum width of woven fabric that can be produced which is caused by a limitation in machine width. Current weaving machines also produce too much noise pollution which may cause damage to the operator's ears. These set maximums and limitations have led us to seek an alternative method to insert weft yarns into fabrics.

In this study, electromagnetic force is being used as an alternative method for inserting weft yarn. In order to accomplish this, an electromagnetic launcher called a coil gun is used to launch a ferromagnetic projectile which would carry the weft yarn through the shed of the warp yarns in order to achieve the interlacing necessary to form a woven fabric. It is expected that this new method of weft insertion would reduce the energy costs that are associated with other weaving machines. The proposed design would be able to insert yarns at a higher rate than any of the current systems available in the market. The new system would eliminate the limits imposed on current machines due to a maximum effective machine width being reached. The proposed design would also eliminate the noise pollution associated with current machines due to the fact that the electromagnetic launching system makes very little noise when it is fired.

Acknowledgments

The work presented in this thesis would not have been possible without the help of the

following people: Dr. Sabit Adanur, Dr. Michael Baginski, Dr. Dan Marghitu, Dr. Peter

Schwartz, Ozdes Cermik, Joe Haggerty, Jeff Thompson, David Clarke, Vladimir Quiñones,

Jonathan Grupp, Jeremy Duffey, Dr. Royall Broughton, and Dr. Jerome M. Solberg.

Table of Contents

List of Figures

Chapter 1

Introduction

In the past several years, the textile industry has moved further away from the United States and established a solid base over seas. This is readily apparent in the weaving industry. The United States was once one of the leaders in producing weaving machinery and woven products. Unfortunately, when the shift was made from shuttle weaving machines to shuttle-less weaving machines, the U.S. was unable to adapt quickly enough to the change. This inability to adapt quickly led woven product manufacturers to turn to foreign machine manufacturers to meet their needs. Eventually, this proved to be more expensive than outsourcing the work which led to the weaving industry leaving the U.S. for all intents and purposes. The shift caused by this departure was felt in the entire U.S. economy, especially in rural areas where the communities revolved around the weaving mills.

That being said, the current shuttle-less weaving machines that caused the shift in industry have reached their maximum potential in terms of speed and production rate. There are also limitations that the current methods face. These limitations include a finite maximum width of woven fabric that can be produced. This is caused by a limitation in machine width that a filling yarn insertion system can properly work within. Current weaving machines also have high energy requirements to perform their tasks especially air-jet weaving, which is the most commonly used method in the industry. The current weaving machines are hazardous to their operators though not to the degree that shuttle machines once were. The hazards in current weaving machinery stem from the amount of noise pollution that they are capable of producing.

This noise pollution causes pre-mature hearing loss in the operators that are exposed to it constantly.

This combination of economic factors and limitations has led us to propose a new type of filling insertion system. This new type of filling insertion system is based on the traditional projectile weaving machines, except that the projectile is launched by electromagnetic force. This new machine would offer several notable advantages over conventional weaving machines. One of the advantages that this machine offers would be an increase in insertion speed. This would greatly increase the production rate of woven materials. This machine would also eliminate the limits imposed on fabric width by machine width due to the fact that this launching system can be used to effectively insert filling yarns at any practical width. Another advantage of this new machine is that it would have less energy requirements than the current most common weaving machine, air-jet. This would make producing woven products cheaper. Another beneficial characteristic of this machine is that the launching of the projectile by electromagnetic force is extremely quiet to the point of producing almost no noise at all. This minimizes the hearing risk that the machine operators are placed under while working, which is premature hearing loss. This combination of characteristics would make this machine highly desirable in the manufacturing world.

The original idea for this research involved using an electromagnetic launcher called a rail gun to propel the projectile. This concept was abandoned due to fact that rail guns have a tendency to wear out and fail with some catastrophic results under continual use. Rail guns also require a large power source to charge the rails to the proper degree necessary to launch the projectile. The charging also takes an extended amount of time to occur. The large amount of energy needed to prepare the rail gun for launch means that the projectile will be launched at an

incredible velocity which could lead to catastrophic failure that could have fatal results if the projectile escapes the machine similar to how the old shuttles used to. This combination of factors makes current rail guns unsuitable for use in weaving machines, since durability and quick filling insertion are the main factors in determining the desirability of the machine.

After some discussion, it was decided that a coil gun would be better suited for the needs of our project. A coil gun was recommended due to its reliability and stability. A coil gun can be fired repeatedly due to its inherent durability. They also do not require nearly as much electricity to power them when compared to a rail gun. Coil guns also possess an inherent flexibility which allows them to be modified and adapted to suit the needs of the designer. They are also capable of achieving results comparable to that of a rail gun without the associated risks. This combination of factors makes coil guns uniquely suited for a new weaving machine design, shown in Figure 1. The focus of this thesis is proving that a weaving machine using a coil gun for electromagnetic filling insertion would be feasible.
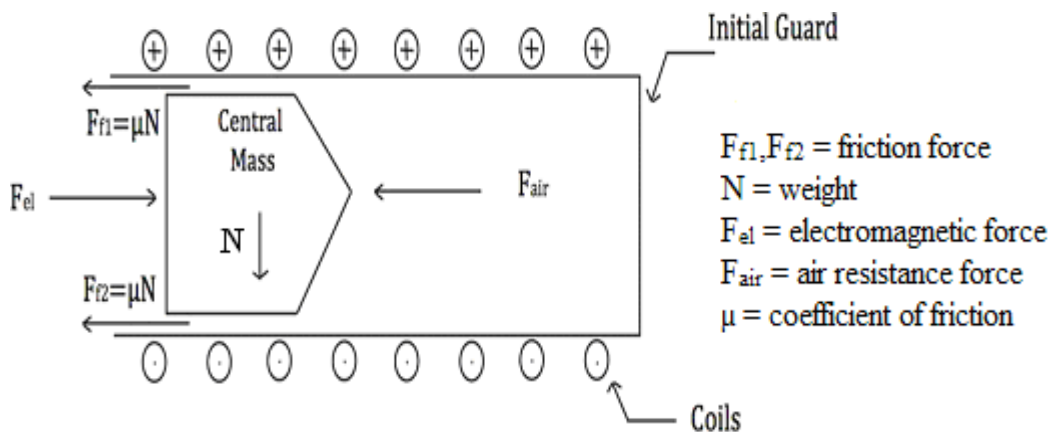
Figure 1: Proposed filling insertion system using electromagnetic propulsion

Chapter 2

Literature Review

Weaving is one of the oldest forms of fabric manufacturing dating as far back as the start of human civilization. This can be said because one of the necessities of life is the need to protect the body from the effects of our environment and to be viewed as more civilized by society. Historians have found evidence that the ancient Egyptians were able to produce woven fabrics more than 6000 years ago while other studies have shown that the Chinese were able to produce fine woven silk fabrics as many as 4000 years ago. Weaving in itself is simply the interlacing of two separate yarns in order to form a cloth or fabric. In weaving, the yarns that run vertically across the produced fabric are called the warp yarns while the yarns that run horizontally across the fabric are the filling yarns. These yarns are capable of being interlaced in different ways in order to form one of many different weave patterns. Weaving was once simply a domestic art and remained that way until the development of the fly shuttle in 1733. This was taken even further with the invention of the first weaving loom in 1745 by de Vaucanson which was improved on by Jacquard who made it possible to control each warp end individually. The first loom designs were followed by the invention of the power loom in 1785 by Cartwright which allowed the entire loom to be controlled from one single point which were later upgraded in the beginning of the 1800's in order to work off steam power. The invention of the power loom led to the need for stronger warp yarn which led to the development of the first sizing machine in 1803 which was one step closer to the first modern weaving machine. By the 1830's, shuttle looms had begun to take over the weaving industry with around 100,000 operating in England

alone. By the early 20th century, the weaving industry was evolved further by new improvements in the winding and warping of yarns leading to the development of warp-tying and drawing-in machines which were another step toward the modern weaving machine. When the World War II ended, the weaving industry began to take its final steps toward achieving the weaving industry we have today (1).

There are many different types of weaving machines available but they all generally fall into one of these types: shuttle, projectile, rapier, air-jet, and water-jet. Despite the fact that there are many different types of weaving machines, they all share some of the same basic features, as shown in Figure 2. These features include the five basic motions of weaving which are warp let-off, warp shedding, filling insertion, filling beat-up, and fabric take-up. The warp let-off and the fabric take-up are the main factors that allow continuous weaving to occur. The first motion of the weaving process is the warp let-off which is used to transport the warp yarns to the weaving machine while ensuring that proper tension is applied to the yarns. The tension in the yarns controls the crimp ratio within the fabric which in turn determines how thick the produced fabric will be. An equal crimp ratio between the warp and filling yarns means that the produced fabric will be thinner while if the ratio is uneven the fabric will be thicker than it needs to be. The warp shedding mechanism is the movement that separates the warp yarns in order to form an opening for the filling yarns to travel through called the shed. The shedding mechanism's opening sequence dictates the interlacing pattern of the final woven product. The warp shedding mechanism is actually made up of two different parts. These parts consist of a metal strip that includes an eye loop for the warp yarns to travel through called the heddle and the harness which the heddle is attached to, which actually controls the movement of the yarns. Each harness controls multiple heddles since each warp yarn in the process has its own heddle it travels

through. This leads to the practice of using multiple harnesses to ensure that the weaving pattern is properly maintained. The number of harnesses used in a weaving machine is determined by the number of different warp yarn patterns that are included in the weaving pattern. Filling insertion is the next of the motions that are necessary for the weaving process to take place. This is the motion in which the filling yarn is introduced into the shed, formed by opening of the warp yarns. Despite the seeming simplicity of this motion of weaving, the filling insertion method determines the classification of the weaving machines. Different types of weaving machines are all named after the filling insertion method that the machine possesses. The next motion in the weaving process is the beat-up. The beat-up motion is performed by a reed which consists of metal dents similar to the teeth of a comb which serves to force filling yarn towards warp yarns to form the intermeshing of the produced woven fabric. The number of dents in the reed as well as the number of yarns that pass through each dent controls the closeness of the yarns in the fabric which in turn controls the thickness of the produced fabric. All these motions lead up to the final motion of weaving which is the take-up motion. The take-up motion is able to control the density of the filling yarns. The five weaving motions must all work together in order for the weaving process to be successful (2).
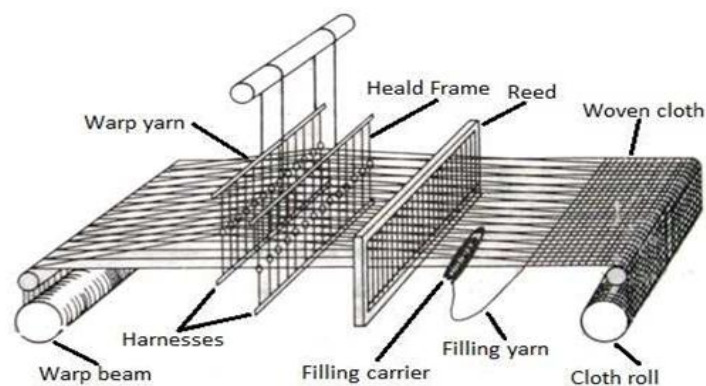
Figure: Basic structure of a loom

Figure 2: The basic structure of a weaving machine (12).

There are different types of weaving machines, but the first type that made its appearance in the textile industry was the shuttle weaving machine. As mentioned before, shuttle weaving machines had begun to come to prominence by the 1830s, with the original design used then not changing much in translation to its modern equivalent. The shuttle weaving machine has been phased out of the modern weaving industry due to the rise of the shuttle-less weaving machines. This decline in the use of shuttle weaving machines and the ceasing of their production is due to the fact that shuttle machines have a number of disadvantages when compared to the shuttle-less variety such as lower speeds which lead to lower production, greater power requirements, greater noise pollution, and the greater risk associated with the operation of these machines. As the name implies, in shuttle weaving, the filling yarns are inserted by a shuttle that travels the width of the machine continuously back and forth, as shown in Figure 3. The shuttle that makes this journey is launched by what is called a "picking stick" that is attached to the sides of the machine. This is accomplished by hitting the shuttle with the stick which causes it to travel across the machine within the open shed. The "picking sticks" themselves are produced from special woods that are meant to absorb energy without experiencing fatigue in order to avoid having accidents during production and ensuring longer life before replacement. During the launching process, the "picking stick" and the shuttle itself journey together for around 20 cm in a process called "picking" after which the "picking stick" ceases to move and the shuttle continues the journey on its own at velocities reaching 50 km/hr. When the shuttle reaches the end of its journey, the other "picking stick" is used to decelerate the shuttle in a process called "checking". There is danger associated with the shuttle weaving machine. This stems from the fact that if the shuttle's flight path is not carefully controlled then the shuttle may exit the shed and fly away from the machine

leading to the injury of the machine operators. Despite the fact that this former backbone of the weaving industry is being phased out, it still holds great importance in today's industry due to the fact that all modern machines are originally based off this first design and incorporate elements of it into their design (1).

Figure 3: Filling insertion mechanism for shuttle weaving (1).

The second type of weaving machine that was introduced into the textile industry was the projectile weaving machine which was introduced in 1952 by the Sulzer company and has the distinction of being the first successful shuttleless weaving machine. This type of machine is capable of manufacturing high quality fabric with minimal energy usage and low cost of production. This type of weaving machine has seen continual improvement and upgrades that have improved its performance over the years. Projectile weaving machines use a projectile to insert the filling yarns in the fabric, as shown in Figure 4, and incorporate a gripper into the design in order for the projectile to hold the yarn. This style of insertion allows the use of almost any type of yarn in the weaving process which gives this type of machine a distinct advantage over the other types of weaving machines. This machine is capable of doing this because the gripper and projectile are able to grip and transport any fiber no matter how course or fine, which allows this machine to produce a great variety of fabrics. The projectile is launched by a "picking lever" which is powered by the energy built up by a torsion bar. The projectile's journey through the shed is facilitated by a rake-shaped guide. Upon reaching the other side of the machine, the

projectile is stopped upon entrance into a receiving device at which point it releases the yarn. Projectile weaving machines have several advantages over the other types of weaving machines. These advantages include low power consumption, less waste of filling materials due to selvage design, quick warp and style changes, reliability and ease of use, easy maintenance, little spare part requirements, and long machine life. This machine also provides the ability to weave more than one width of fabric at a time. Projectile weaving machines are capable of producing multicolor fabrics as long as the sequence of colors stays within four or six different filling yarns. Projectile weaving machines are capable of achieving a maximum insertion rate of 1400 m/min which makes it slower than the jet weaving machines but faster than the other types (1).

Figure 4: Filling insertion mechanism for projectile weaving (1).

A third type of weaving machine that was introduced to the textile industry was the rapier weaving machine. The insertion method for this type of weaving machine consists of either a flexible or rigid element known as the rapier which carries the yarn across the shed. During the insertion process, the head of the rapier grabs the yarn and carries it through the shed. Upon reaching the other side, the rapier head releases the yarn and returns to its original position in order to pick up the next yarn for insertion. There are two distinct types of rapier machines that are currently available on the market, as shown in Figure 5: rigid rapier and flexible rapier machines. In rigid rapier machines there is only one rapier which is designed to be rigid and at least the width of the machine that it is being used on. These single rapiers are manufactured from either metal or composite bars that have a circular cross-section and high mass in order to

ensure that the rapier travels a straight path through the shed. In this version of the machine, the rapier enters the shed from the end opposite the filling yarn, travels through the shed, grabs the filling yarn and then retracts while carrying the yarn through the shed. This allows the rapier to only move the yarn in one direction which causes a large amount of wasted movement within this machine. On the plus side, the single rapier with no yarn transfer allows the machine to be highly desirable for fabrics that have filling yarns that are unwieldy. This machine is the less popular of the two types of rapier weaving machines. In flexible rapier machines there are two rapiers that work together to carry out the yarn insertion. In this type of rapier weaving machine, one rapier which is termed "the giver" transports the filling yarn through the shed to the middle of the machine where it transfers the yarn to the second rapier termed "the taker" which retracts and brings the filling yarn the rest of the way through the shed. This version of the machine suffers from the problem of a large amount of the rapier's motion being wasted. Rigid rapier weaving machines suffer from the fact that they require a large amount of space because the length of the rapier is extended outside the machine when the rapier is retracted. This however, is not a problem in the flexible double rapier weaving machine since the rapier is made of a tape-like structure that can be wound into a barrel structure in order to save space. Rapier weaving machines have gained the reputation for being among the most reliable and versatile of the different weaving machines. They are capable of weaving both light-weight and heavy-weight yarns. Rapier weaving machines are capable of achieving weft insertion speeds of around 1260 m/min which makes this machine slower than jet weaving machines but comparable with the projectile machines (1).
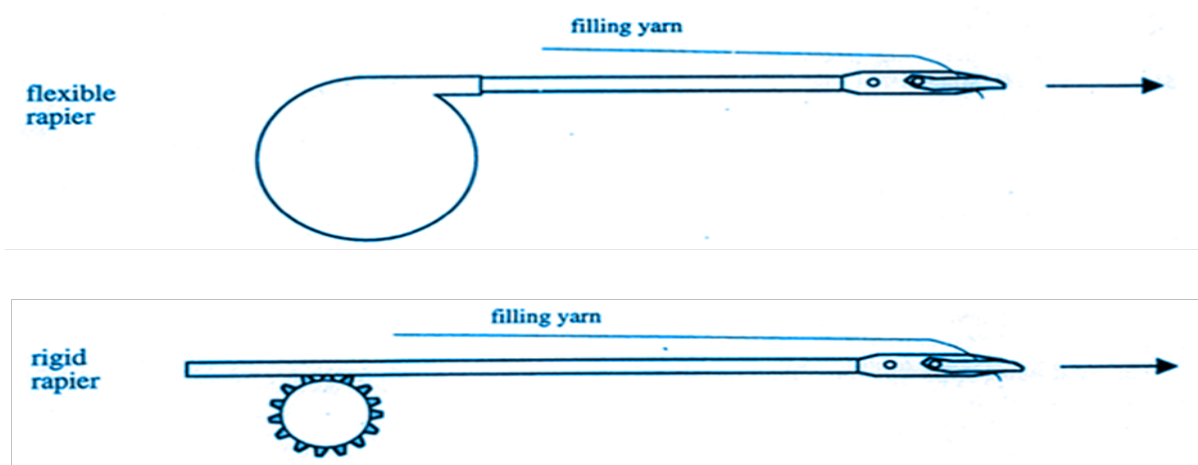
Figure 5: The two different types of filling insertion mechanism for rapier weaving (1).

The next type of weaving machine introduced to the textile industry was the air-jet weaving machine which was introduced by Paabo in Sweden in 1951 and is currently the most productive machine available. Like the other weaving machines the name indicates how the filling yarns are inserted into the shed, which in this case, is with the use of compressed air, as shown in Figure 6. During the filling yarn insertion process, yarn is first drawn in from a package containing the filling yarn supply by what is called a "filling feeder" and each pick drawn in is measured in order to ensure proper insertion by a "stopper". After the "stopper" releases the correct amount of filling yarn, it is then transferred into the "reed tunnel" through the combined efforts of the tandem and main air nozzles, which provide the initial propulsion; then, the relay nozzles across the machine are used to maintain a high air speed throughout the shed. In order to ensure a proper flight path for the yarn and to prevent intermingling of the warp and filling yarns during flight, a profiled reed is used. Once the filling yarn reaches the other side of the shed, it is cut in order to begin the insertion of the next filling yarn. A major advantage of the air-jet weaving machine is that it provides high production rates. This makes these machines ideal for the cheap production of standard fabrics in wide array of styles. This does not mean that

air-jet machines are limited to this nitch, since the machines are also capable of producing heavy cotton fabrics as well as other specialty fabrics. The insertion method for this machine is easily the simplest out of all the filling insertion methods which has led to some of its popularity in the industry today. The simplicity of this design is exemplified by the fact that there are only a few major components which include tandem and main nozzles, ABS brake system, and relay nozzles all of which are simple designs. The fact that the mass of the insertion media is rather small compared to that of the other mentioned types of weaving machines contributes to the higher obtainable speeds that this machine is capable of. Air jet weaving machines also benefit from a lack of mechanically moving parts during the insertion step, unlike rapier or projectile weaving, which allows a higher insertion speed to be reached by the machine. Air-jet weaving machines offer several other advantages over the other types of weaving machines some of which include "high productivity, low initial outlay, high filling insertion rates, simple operation and reduced hazard because of few moving parts, reduced space requirements, low noise and vibration levels, low spare parts requirement, and reliability and minimum maintenance (1)." This type of weaving machine is capable of reaching a filling insertion rate of up to 2400 m/min in the commercial industry while using up to eight different colored yarns. Although this speed is the highest achievable in a commercial setting, laboratory settings have shown the machines are capable of reaching speeds of up to 1800 ppm. This speed capability allows air-jet weaving machines to outperform the other types of weaving machines (1).

Figure 6: Filling insertion mechanism for air-jet weaving (1).

The final type of weaving machine that was introduced to the textile industry was the water-jet weaving machine which was introduced in 1955 at the Brussels Textile Machinery Exhibition by Vladimir Svaty. As with the other types of weaving machines, the name of this machine implies how the filling yarn is inserted into the fabric, which in this case, is a high pressure jet of water, as shown in Figure 7. This type of filling insertion is possible only when the velocity between the filling yarn and jet of water is different in order to add tension to the yarn. If this differential is not present during the insertion process, then curling or snarling could occur in the filling yarn due to the lack of tension. The traction force that is needed to carry the yarn with the water jet can be controlled by both the length and roughness of the filling yarn being inserted and the inherent viscosity of the water which is controlled by temperature. Higher viscosity waters are capable of creating higher traction forces between the filling yarn and the water. Regardless of the viscosity of the water, the traction force will not be sufficient if the filling yarn itself is not wettable. The water that is used to insert the filling yarn goes through a three phase flow process during each insertion step. During the first stage of flow, the water is accelerated within the pump before being introduced into the nozzle. The second stage of flow involves the water being expulsed through the nozzle in the form of a pressurized jet. The third stage of water flow is the flow of the water within the shed which is conical in shape with three distinct regions: compact, split, and atomized. Filling insertion is better performed by the compact and split regions of the water flow. In order to insure accurate filling insertion, the nozzle that the water flows from has to be adjusted upward in order to account for the parabolic arc of the water as it flows through the shed. After the filling yarn has reached the end of the shed, it is stopped by the reed of the machine without the need for additional equipment. Water-jet weaving offers some advantages over its closest contemporary, air-jet weaving. One of the

advantages is that the water provides longer propulsion of the filling yarn due to the greater coherency of the water. Also, due to the greater mass of the water, the filling yarn is less likely to become entangled with the warp yarns. The machine also has greater stability than air-jet weaving machines due to the fact that the water pump and the picking mechanism are attached to the machine in order to ensure that the beat-up mechanism only moves the reed which prevents having to recalibrate the nozzle for each insertion. Water-jet machines are not without their own unique disadvantages which include the fact that the filling yarns must be dried after insertion and the waste water has to be disposed of after insertion as well. The width of a water-jet machine is entirely dependent on both the pressure and diameter of the water jet. Typically the diameter of the water jet is approximately 0.1 cm and the amount of water used during insertion is smaller than 2 cc. Supplying the appropriate pressure for the machine width is usually not a problem due to water's incompressibility. Some recent additions to water-jet machines have allowed the use of multiple different filling yarns (up to four) through the incorporation of multiple pumps and nozzles. Water-jet machines have a maximum speed of around 1,500 ppm with a 3 m wide reed and a filling insertion rate of 1800 mpm (1).
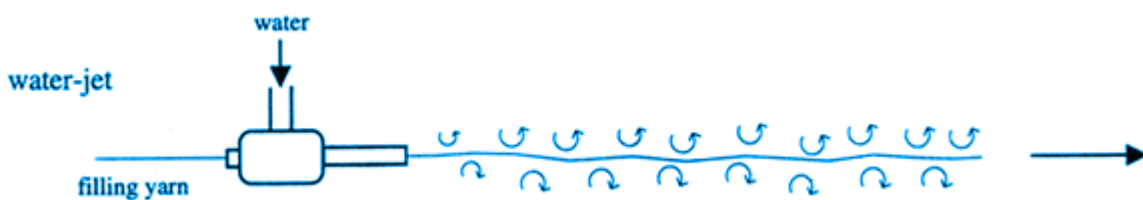
Figure 7: Filling insertion mechanism for water-jet weaving (1).

There have been two previous attempts at developing a weaving machine that is based on projectile weaving that uses electromagnetic force to launch the projectile rather than traditional means. The first of these attempts was designed and constructed by Rohit Verma who filed for a

patent on April 7, 2004, which was granted on October 20, 2005 (11). Verma's design incorporates not only the filling insertion mechanism but the shedding system as well. Both of these concepts suggest an electromagnetic levitation and propulsion method. The mechanism for shedding is carried out through the used of an electromagnet placed in the middle of the harnesses. The electromagnet causes the harnesses to levitate and be propelled in opposite directions in order to open the shed. This levitation is made possible by the fact that the harnesses themselves have electromagnets placed on them in such away that all directions are covered by the magnets. These magnets work in concert with the middle magnet and a bolt-type pin system to control how the shed is opened. The pins used for this have magnets on their heads to help with control of the harnesses. The filling insertion mechanism is carried out through a magnetic levitation tunnel that serves as the reed of the weaving machine. The carrier for the weft yarn is levitated and accelerated through the tunnel by the electromagnets within the tunnel until it reaches the other end at which point it is decelerated by the electromagnets on the other side, shown in Figure 8. The insertion mechanism design also incorporates a "drop pin" that falls to indicate when a warp yarn has broken. The "drop pin" works in concert with a sensor laser to accurately determine when a break occurs. The design of this weaving machine includes a customized particle image velocimetry gear box that allows the picks per unit length to be controlled automatically through the use of a microprocessor. This machine is capable of achieving a filling insertion rate of 1000 meters per minute with a picking speed of 4800 picks per minute. This, however, has only been accomplished for a 165 cm wide loom (11).
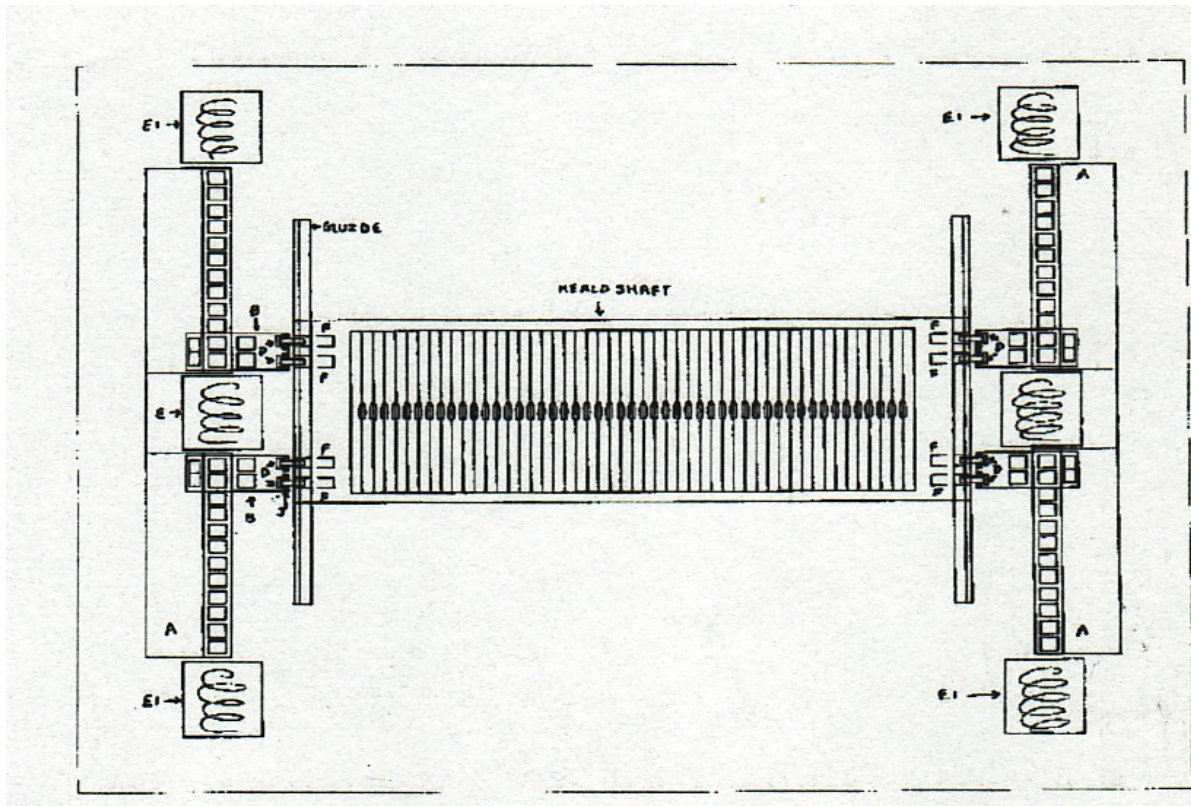
Figure 8: Electromagnetic weaving machine by Verma (11).

The second attempt to develop an electromagnetic weaving machine was carried out in

Yazd, Iran with results published in July 2005 (10). This weaving machine design launches the

projectile carrying the filling yarn using non-stroke electromagnetic propulsion. The launching

system for this weaving machine uses a solenoid to provide the electromagnetic field needed to

propel the projectile, shown in Figure 9. The aim of this system was to establish the insertion

system while maintaining the simplicity of the machine design. This machine was designed to

meet certain predetermined goals. One of these goals was to reach the current maximum

acceleration of the filling projectile in weaving machines that are in use which is 7,000-11,000

m/s^2. Another goal for this design was to achieve an acceleration time of approximately 0.007

sec which is typical of standard projectile weaving machines. A third goal that this design hoped

to achieve was to make the projectile travel the typical distance required in current projectile machines which is 6-7 cm. The final goal of this design was to achieve a final speed for the projectile of approximately 20 to 25 m/sec. The end result of this project was a functional version of the machine. Despite the fact that a functional machine was produced, all of the goals of the project were not met. The main goal that was missed for this machine was the speed of 20-25 m/s, since the maximum speed obtained from their machine was only 5.70 m/s. The developers of this design feel that the design will work with more in depth research and development (10).
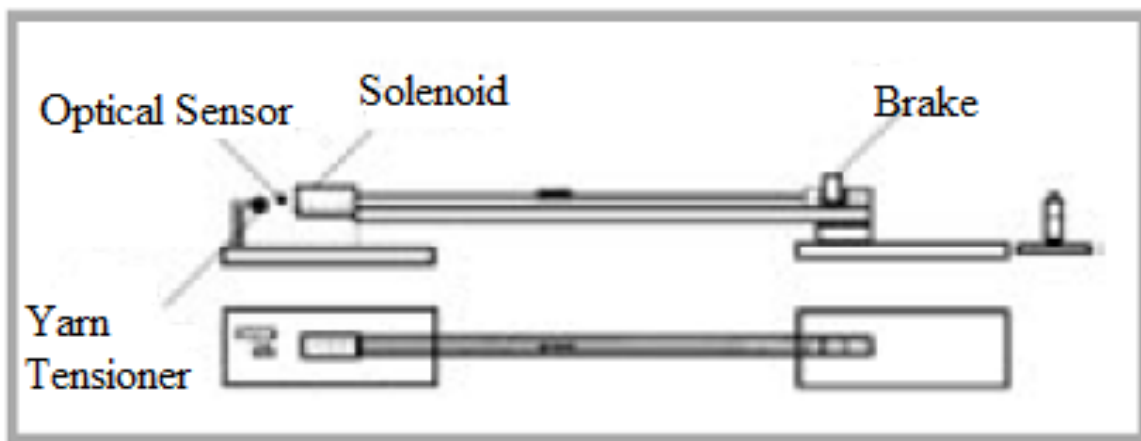
Figure 9: The insertion mechanism for the Iranian machine (10).

Another field that is seeing constant innovations and improvements is the field of electromagnetic launchers. Although this field has seen periodic spikes of interest and research over the years, it wasn't until 1972 that there was significant growth in the technologies needed to support the development of improved electromagnetic launchers. After 1972, many new developments have been made and research into this field has seen constant attention. This research has spawned the Japanese bullet train which uses electromagnetism to levitate above the

17

tracks and help propel it at high speeds. The research in this field first involved the production of a linear induction motor in order to provide propulsion. However, it was ultimately proven to be insufficient in providing the necessary propulsion to launch. This early research was essential in the creation of the linear synchronous motor which evolved from the original design of the linear induction motor. This new type of electromagnetic motor was shown to be able to provide sufficient propulsion necessary for launch. This motor was so successful that NASA researchers have incorporated it into the design of a mass driver, a type of electromagnetic catapult, which could theoretically eliminate the need for the initial propulsion rockets in space shuttle launches. Currently, a new improved version of the mass driver is being designed and constructed at Princeton and MIT (9).

The field of electromagnetic launchers is an ever expanding field, but by far the most developed of these launchers is also the simplest the railgun. The basic design of a railgun incorporates two rails situated parallel to each other that are connected to a dc current source. Between these rails lies the projectile which is made up of a short-circuit slide propelled along the rails through the power of the Lorentz force. The railgun itself has been subjected to intense study by NASA as well as the aforementioned research by Marshall and Barber (9). Railguns have the ability to operate in two different modes. One of these modes is the distinction brush conduction mode. This is the standard mode that railguns operate on using just the current in the rails to provide the propulsion for the projectile. The other type of mode that a railgun can operate in is the metallic conduction mode. In this mode, the current flows through the sliding projectile itself which allows it to launch a 1 kg mass at an acceleration of up to a speed of around 2,000 g through the use of a switching gun in order to power the main railgun. Through their research Marshall and Barber discovered that if too much stress is placed upon the railgun,

a plasma arc is produced that bypasses the projectile causing the proper acceleration to not be reached. They countered this effect by creating a projectile made out of the non-conducting material lexan and by trapping the plasma arc behind the projectile. Using this modification, Marshall and Barber were able to accelerate the projectile at a much faster rate than the traditional method. When the projectiles being launched increase in size, it is predicted that the standard method of distinction brush conduction combined with plasma conduction will fall by the wayside and be replaced by a combination of brush conduction and arc conduction (9).

The practical limits of railguns have not yet been fully explored in terms of projectile size, acceleration, length and velocity, but they can be examined through further developments in the materials and engineering going into the design of a railgun. Marshall and Barber's work has provided enough results in order to justify further research into this field. Despite evolving research in this field there are two other limiting factors that must be taken into account when determining the practical limits of the railgun: acceptable cost and service life. Service life is especially important as containing the expansion forces of the railgun put a lot of stress on the rails which can cause the rails to blow apart. This can cause problems in both the electric current and the constant pressure that is kept within the barrel of the gun. Another factor in the service life of a railgun is the destructive effect of high density brush current which can severely damage the railgun during repeated uses. Despite this, insufficient research has been undertaken to determine exactly how much of an effect the high density brush current will have. In addition to these limiting factors, railguns also suffer from the limits imposed by both the maximum length of the barrel and the muzzle velocity. This is especially evident in the barrel length since as it increases much of the energy used to accelerate the projectile is absorbed by the resistance and inductance inherent to the rails which is magnified by the length the projectile must travel down.

Firing the projectile at a greater velocity also has a detrimental effect on the amount of energy that can put into the projectile as well. This is related to the amount of voltage that is needed to launch a projectile at a higher velocity since there is a limit to how much voltage can be contained within the gap between the rails. These limits effectively restrict the amount of energy that can be transferred into the projectile despite the availability of it (9).

Another form of electromagnetic launcher that is of a much simpler design than a rail gun is a coil gun. In this type of launcher, a ferromagnetic projectile is accelerated down a tube that is the barrel of the gun. In order to achieve acceleration, the tube is encased in multiple coils of a magnetic material that creates a solenoid similar to what is used in a rail gun. The coils are used to create a magnetic attraction between the projectile and the coil which propels the projectile at a rapidly increasing speed. This launching mechanism makes a coil gun a perfect example of a solenoid that does not have any limits placed upon it. This type of electromagnetic launcher is incredibly powerful despite having a simple design that features no moving parts. This design also allows for repeated usage due to the fact that there are no parts that can wear out making the launcher incredibly durable. Projectiles fired from this launcher produce no extra effects such as fire, flash, or sound which makes this type of launcher incredibly quiet (6).

Chapter 3

Experimental Set-up and Measurements

The research was begun by searching YouTube for examples of coil guns. The search led to a video posted by Homemade Innovations that demonstrated how a basic coil gun could be made using a disposable camera. Following the included link in the video, the Homemade Innovations website was reached which included more detailed written instructions on how to develop the coil gun as well as having the YouTube video to watch for instructions. Using the instructions provided by the webpage as a guide, the items necessary to construct the coil gun were obtained (8).

3.1 First Prototype-Materials

The first item that was acquired was a Kodak disposable camera, as shown in Figure 10, which was acquired from the Auburn Bookstore. The camera is needed to provide the necessary circuitry to power the coil gun. The flash circuit from a disposable camera is a perfect starting point for assembling a coil gun. This is because the flash circuitry includes both a 330 volt, 120 micro-farad capacitor as well as a button to charge it and a 1.5 volt AA battery to provide the power needed to charge the capacitor. This saved us from having to build any complicated circuitry that we are unfamiliar with due to our lack of an extensive electrical background.

Figure 10: A typical Kodak disposable camera with power flash (7)

Some 20 gauge multi-strand coated copper wire was then acquired, shown in Figure 11, from one of the lab technicians in the Polymer and Fiber Engineering Department. It is important that the wire be copper in order to insure that proper conduction can be achieved. The wire served a variety of different purposes in the coil gun design. The most important purpose that the wire served in the coil gun is forming the coil used to provide the acceleration necessary to launch the projectile. The wire also served as the connector for the different components of the coil gun.
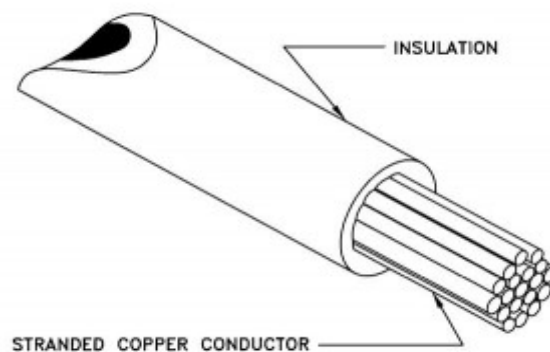

Figure 11: The design of multi-strand coated copper wire (13)

Several other items were also obtained to serve as additional components in the coil gun, as shown in Figure 12. One of these items was a standard ball-point pen which, after some modification would serve as the 12.07 cm long barrel of the coil gun. A lab tech in the Polymer and Fiber Engineering Department was able to acquire another item for use in the construction of the coil gun which was a push button switch that would normally be used to start an all-terrain vehicle. Electrical tape was also acquired to be used as both a spacing tool as well as to protect the connections of the wires used to connect the different components of the coil gun. It was also decided to acquire an 8d 2-1/2" bright common nail and cut it into smaller pieces having a mass of 1.0137 grams to serve as the projectiles for the gun due to their inherent ferromagnetic properties.

Figure 12: The remaining items needed to construct the coil gun (3,4)

3.2 First Prototype-Construction

The first step of constructing the first prototype of the coil gun was to remove the battery and outer shell of the Kodak disposable camera. This was attempted several times before the camera was taken to a lab technician in the department with experience working with electrical components, to safely remove the battery in order to avoid getting shocked by the camera. The technician was able to remove the battery without any incident and showed how to properly remove the casing of the camera. After the instruction, the outer shell of the camera was

successfully removed revealing the inner circuitry that powers the flash. Unfortunately, when

attempting to remove the battery and the outer shell, the flash button was pressed; a charge was

present within the capacitor which caused a shock when it was touched. In order to avoid a

repeat of this event, the capacitor had to be manually discharged. This was done by

simultaneously touching the nodes of the capacitor with a flat head screwdriver. After the

capacitor was discharged, the flash was removed from the circuit, as shown in Figure 13, through

the use of a pair of needle nose pliers.
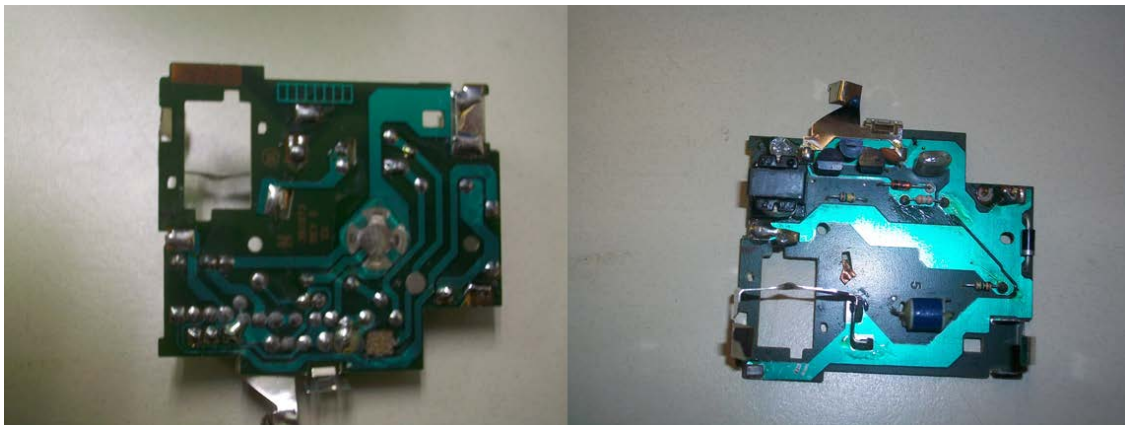
Figure 13: Front and rear view of the flash circuit from the Kodak disposable camera after flash removal.

The ball-point pen was disassembled to use the pen tube as the barrel of the coil gun. The

electrical tape was then used to form an area for the conductive wire to be wrapped around the

pen tube in order to complete the coil gun barrel. This was done by wrapping the tape 2.54 cm

from one end of the pen tube. A second wrapping was added after the first, leaving a 2.54 cm gap

between the two in order to guide the wrapping of the wire on the tube. The space between the

sections was then wrapped with the coated 20 gauge wire. This required a great deal of precision

in order to ensure that the coils of wire stay on the pen tube making this the most time

consuming section of the prototype construction. Sections of the wire at the beginning and end were allowed to extend off the tube in order to make the necessary connections to the other components of the gun. One end of the wire was connected to the push button switch. The other end of the wire was connected to one of the nodes of the capacitor in the flash circuit. Another section of wire was used to attach the other node of the capacitor to the other input of the switch. The coating had to be stripped from each end of the multi-strand wire in order to make the connections. Once all these connections were made, the circuit was complete and the first prototype coil gun was complete. However, upon inspection of the completed coil gun it was discovered that the flash circuit was not physically attached to the battery port. A technician in the electrical engineering department was consulted after this discovery was made. The technician could not correct this problem either without a schematic of the circuit, so it was decided to get another type of camera in order to obtain a circuit with the battery port intact.

3.3 Second Prototype-Materials

While in contact with the electrical engineering technician, a more suitable 20 gauge copper single strand wire was obtained, as shown in Figure 14, to make the coil with. This type of wire was more suitable since we would not have to remove the coating from the wire in order to make any connections possible. This new wire was also beneficial to work with since it was easier to manipulate one strand of wire rather than multiple strands to make the coil. The multi-strand was also kept to make some connections due to the limited amount of the single strand wire we had to work with. A new disposable camera was acquired from Wal Mart which was made by Fujifilm.

Figure 14: The single strand 20 gauge copper wire.

3.4 Second Prototype-Construction

The construction of the second prototype began in the same manner that construction of the first did with the removal of the battery and outer shell of the disposable camera. The battery was easily removed from this disposable camera due to a convenient access panel. The removal of the outer shell was an easy process due to the experience from the first prototype. Fortunately, no one was shocked when the flash circuit was removed from this camera, shown in Figure 15; the battery port was attached to it.
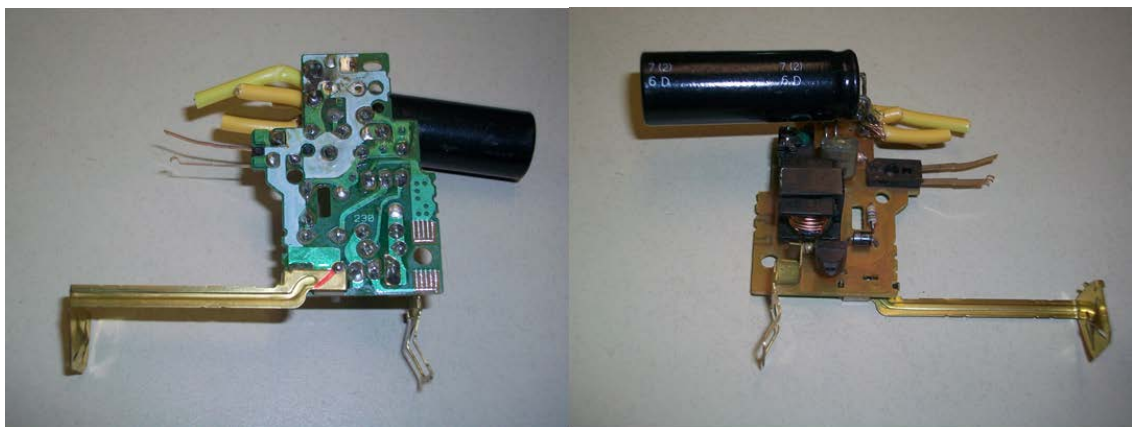

Figure 15: Front and rear view of the flash circuit of a Fujifilm disposable camera with the flash removed

While the battery and the outer shell of the camera were removed, the previous barrel was deconstructed. Once the multi-strand wire was removed from the barrel, the single strand wire was wrapped around the pen tube. Despite the fact that the single strand wire was easier to work with than the multi-strand, this was still a slow process due to the precision needed to ensure the wire stayed in place. The barrel was then connected to the other components of the gun using the same method as the first prototype except instead of letting the single strand wire connect directly to the switch or capacitor; we used the multi-strand wire in order to conserve the single strand. Using the multi-strand wire as a connector meant that it had to wrap around the ends of the single strand wire. Once this was accomplished, the connection between the multi-strand wire and single strand wire was covered in electrical tape to ensure safety in the device. When the proper connections were made, the battery was reinserted into the circuit and a piece of copper that served as the flash charge button was used to close the circuit so that the capacitor would charge. The initial capacitor charging was successful, so we manually discharged the capacitor without the battery in the circuit and repeated the process a few more times to ensure it would work multiple times. Unfortunately, during one of the manual discharges the battery was not removed from the circuit and a transistor within the system was burned out. This caused a noticeable increase in temperature around the transistor and produced a distinctive odor. After some analysis from using a volt meter, it was decided to use a brand new circuit rather than attempt to replace the burnt transistor.

3.5 Third Prototype

The third attempt at producing a working prototype of a coil gun was done using a Cannon non-disposable camera that was acquired from a yard sale in the hopes that the circuitry would be sturdier than that of a disposable camera. However, this attempt failed, since the outer shell of the non-disposable was much more difficult to remove than that of the disposable camera. Additionally, when the outer shell of the camera was removed, it was discovered that the circuitry in the Cannon, as shown in Figure 16, was too complicated to figure out. Complicating matters further was the fact that the battery port did not seem to be removable with the flash circuit. Taking this into account, it was decided to return to using only disposable cameras in the prototype construction.
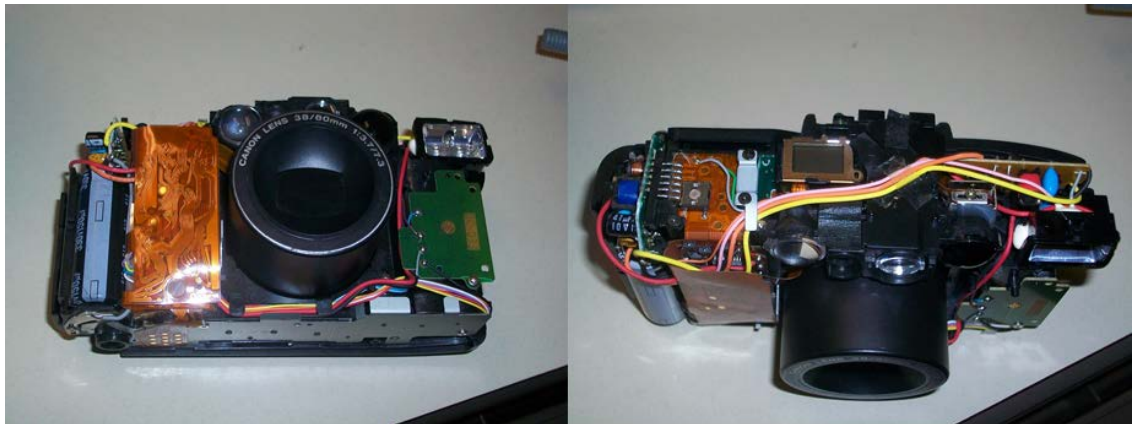

Figure 16: Front and top view of the flash circuitry of a Canon non-disposable camera

3.6 Fourth Prototype

Following the attempt at using a non-disposable camera, it was decided to give the Fujifilm disposable camera another try for our fourth attempt at developing a working prototype. Following the same steps that were used to make the second coil gun, the newest prototype of the

coil gun was constructed. Following the construction of this prototype, a test shot was attempted. The acceleration of the projectile did not occur when the button was depressed after the capacitor had been charged. After the failed shot, the prototype was taken for analysis. Upon inspection of the prototype, it was pointed out that the flash had not been removed from the circuit which would lead to a conflict with the coil when the capacitor was discharged. While the electrical engineering technician removed the flash from the circuit, the video that was used as a guide to construct the coil gun was reviewed. After viewing the video, it was determined that some of the steps presented in the video had been overlooked or inaccurately done. One of the things that was noticed as inaccurate in the design was that there was not enough coils of wire on the barrel of our gun and that the tape used to designate the area that the wire would be placed should be duct tape rather than electrical tape so that it would be easier to add a required 1.27 cm of diameter to the barrel of the gun that had previously went unnoticed in the instructions. In order to implement these changes to the prototype design, the original barrel had to be deconstructed again. Then starting with the original pen tube, duct tape was wrapped 2.54 cm from the end of the tube until the desired increase in diameter was achieved. This process was repeated leaving a 2.54 cm gap between the two pieces of tape. During the wrapping process, the duct tape had to be cut in half in order to avoid covering the entire tube without having room to leave the necessary gap for the wire. Once the increase in diameter was achieved, the single strand 20 gauge wire was slowly and precisely wrapped around the pen tube until it reached the same diameter as the tape. Since this was such a slow process, duties were exchanged at one point which led to some inconsistencies in the coil partly due to the change in winding and partly due to the size of the coil which made the top lair of the wire not as uniformly tight as the rest of the coil. Another problem that was noticed in the design when compared to the video was that the

29

coil gun in the video used the combined capacitance of twenty of the capacitors from the flash circuit of disposable cameras wired together in a perpendicular manner. In order to simulate this effect, the electrical technician was asked to solder a 1000 microfarad capacitor with a maximum allowable voltage of 400 volts into the circuit parallel to the disposable camera capacitor. The technician also soldered the connections from the barrel to the capacitor and the button, which remained the same as the previous prototype attempts, in order to ensure a good connection between the components while reducing the chance of unnecessary sparks during firing.

The completed prototype was taken to a lab in the Electrical Engineering building so a voltmeter could be used for analysis. The voltmeter was used to monitor the charging of the capacitors as the circuit was closed using the copper flash control. Once a voltage of around 180 volts was achieved, the projectile was loaded into the barrel of the gun and positioned so that it was surrounded by the coil in an attempt to test fire the prototype. The test shot was successful but attempts to replicate the effect were unsuccessful. After attempting to charge and fire the gun several more times, a rather pungent odor was noticed coming from the circuit similar to the smell from our previous circuit that burned out a transistor. Using this evidence and the reading from the voltmeter, it was concluded that another transistor had been burned out. Upon this discovery, it was decided that an additional switch was needed in the circuit to eliminate the backflow of current through the flash current during discharge of the capacitors.

3.7 Fifth Prototype

The fifth prototype design took the basic design proven to work in the fourth prototype and incorporated a few modifications to prevent the transistor destruction that occurred in the previous design. One of the major modifications to the design that was implemented was to

incorporate another switch into the circuit to prevent the current from feeding back through the flash circuit when the capacitors discharge. The original idea was to simply add another switch into the circuit, but an alternative method was provided upon consultation with the electrical engineering technician. The alternative method involved replacing the button that was previously used with a different switch that had the ability to function as two different switches with one press of a button. When this new button was pressed, it created an open circuit between the 1000 micro-farad capacitor and the flash circuit and created a closed circuit between that same capacitor and the coil gun. This allows the capacitor to be discharged safely without fear that it will burn out the transistor again. In order to further protect the flash circuit from the discharge of the capacitor and to increase the efficiency of the discharge into the coil, a diode was added into the circuit where the connection to the coil occurs. This prototype, shown in Figure 17, has been successfully fired many times and will be the system used for a majority of the testing process. As a point of interest, it was noticed that the secondary capacitor does not charge if the voltage on the capacitor in the flash circuit reaches too high of a level. This requires the flash circuit capacitor to be discharged in between firings at times.

Figure 17: The completed fifth coil gun prototype.

3.8 Testing

The coil gun was tested by using a high-speed camera in the Polymer and Fiber Engineering Department. The services of a former graduate student in the department who has experience using the camera were enlisted to teach how the camera could be properly used to test the coil gun. The initial test was setup in order to learn how to use the camera, so there were not any test parameters specified. The barrel of the coil gun was lined up with the lens of the camera. A set of lights was used to provide enough light for the camera to pick up the projectile on the computer screen. The gun was fired twice using this initial setup in order to demonstrate how the camera system worked. These initial test shots also demonstrated that the projectile needed to have some sort of contrast on it so that the camera could automatically track and record data on its flight.

The second set of tests was carried out using projectiles that had been marked with a white-out pen in order make a narrow line that stretched the entire diameter of the projectile. It was hoped that this line would cause the necessary contrast with the surface of the projectile so that the camera would be able to automatically track its flight. A white piece of board was also added as a background for the light to bounce off to provide better illumination for our test. Unfortunately, the added preparation of the projectiles did not pay off since the camera still could not pick up enough contrast between the white-out and the projectile to be able to track the projectile automatically. In order to provide the necessary contrast, it was suggested that a method using an alternating white and black circular symbol to create the necessary contrast should be tried.

In order to carry out the third set of tests, it was decided to modify the suggested method to produce the contrast in the projectile by painting the entire projectile black and then adding the white-out line to them. However, the attempts to spray paint the nails were ineffective due to the galvanized coatings present on the nails. In the meantime, a new light source was obtained to replace the previously used light source which had become unavailable for use. Some reflective tape was also acquired in the hope that the light would reflect off the projectile making it easier to track on the camera. A small strip of the reflective tape was wrapped around the unsuccessfully painted projectile. The same setup was used for these tests except the white background was replaced with a black one. After a failed attempt at using the black background, the white background was reused, shown in Figure 18. Even with the combination of the reflective tape and the new brighter lighting system, the camera still could not track the projectile automatically.

Figure 18: One of the initial testing setups

Following the failure of the camera to automatically track the projectile in the previous set of tests, we began preparing for our fourth set of tests. During the preparation for this set of

tests, the nail was successfully spray-painted after numerous attempts to find the proper level of sanding to remove the galvanized coating from the nail. A Mechanical Engineering student was contacted in order to obtain some help setting up the lighting properly and explaining how to manually track the projectile properly. With the student's help and the use of a white foam board background, shown in Figure 19, some tests that produced usable data were able to be carried out. A shot was fired using a shutter speed of 2000 frames per second and a contrast of 1/5000 over a distance of 20.32 cm. The voltage that the projectile was fired at was not recorded since this was a test shot. Using this new testing setup, the shot distance was increased to 25.4 cm and decreased the shutter speed of the camera to 500 frames per second and began to perform our tests. Five different shots were performed under these test conditions. Four more shots were performed across a span of 22.86 cm.

Figure 19: Final test setup

Chapter 4

Results and Discussion

4.1 Test Shot

The first shot that results were recorded for was the test shot that was fired in the presence of the mechanical engineering student. Unfortunately, since this was only a test shot to determine if the camera would record the projectile correctly, an accurate recording of the voltage the projectile was fired at was not made. It was assumed that the shot was made around 186 volts based on the recollection of the firer. The results recorded were in terms of bits, so they had to be converted to cm. This was accomplished by an automatic conversion factor that was generated by the camera when the span was given in the preparation for the shot. This conversion factor was given as 1 bit = 0.05404 cm.

The average velocity of the test shot was 36.95 m/s. The acceleration in the barrel of the coil gun for this shot was calculated to be 11,316.22 m/s^2. Using this information the percent efficiency of the coil gun was calculated using the following equation:

$$\% \, Efficiency = \frac{m * Vo^2}{c * V^2} * 100$$

where,

m = mass of projectile in kg

Vo = the initial velocity of the projectile in m/s = calculated average velocity

c = capacitance of the capacitors in Farads

V = the voltage the projectile was fired at in volts

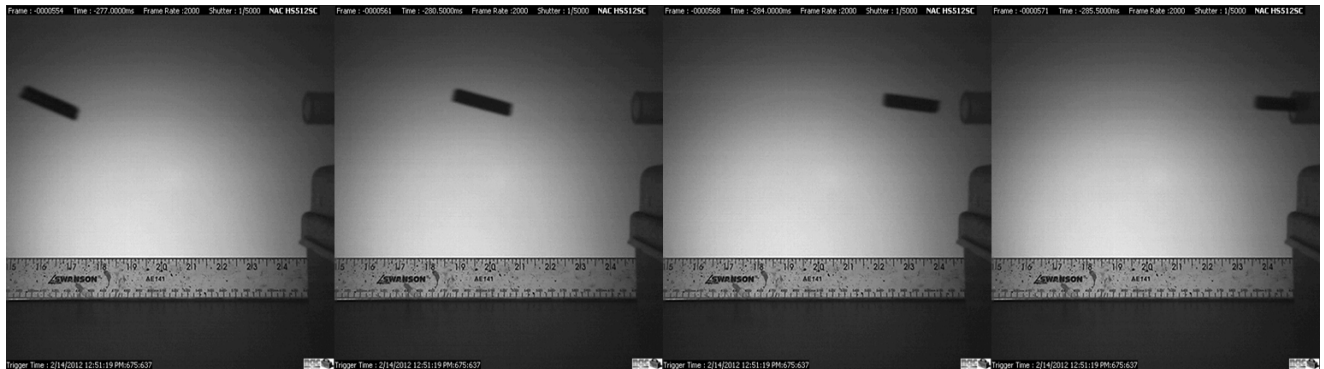The % efficiency of this shot was calculated to be 3.57%.

Figure 20: The flight path of the test shot.

The visual data presented in the still frames of the video of the test shot, shown in Figure 20, show an interesting phenomenon in the flight of the projectile. The phenomenon that is visible is the fact that the tip of the projectile tilts up in the air in flight. This is similar to a boat pushing a wake at high speed.
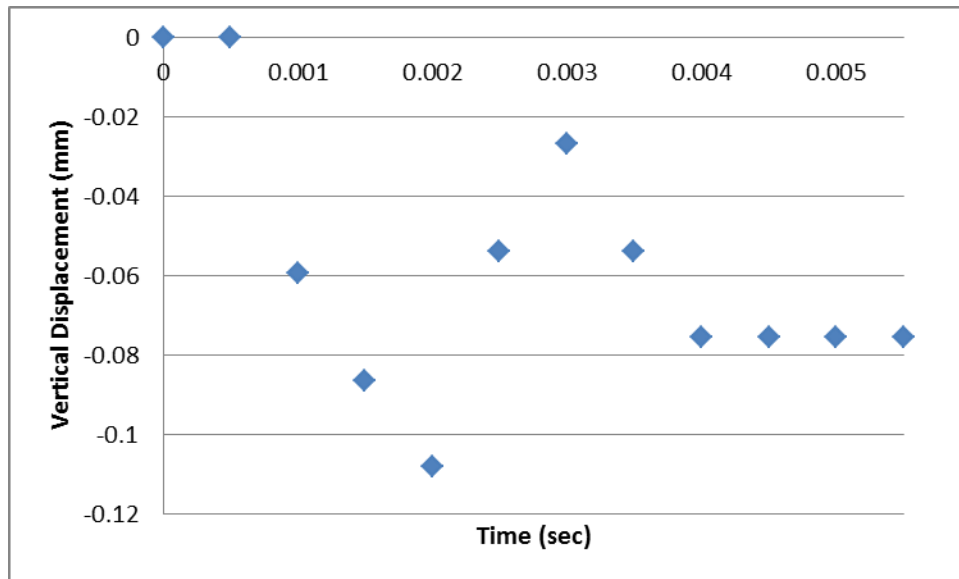

Figure 21: Loss of altitude of the projectile with time for the test shot.

As shown in Figure 21, the vertical displacement of the projectile during flight is inconsistent over time. This is evident in the fact that, at one interval of time, the information implies that the projectile experienced a climb in altitude. There are two reasons that this may happen in the results. The first reason is that the method that was used to obtain the measurements depends on the auto tracking feature of the camera losing track of the projectile so that a new data point can be designated for measurement. While this method can lead to inaccuracies, it should not account for a large section of altitude gain. The second reason that there is an increase in altitude in the results is that the upward tilt shown in the projectile affected the results for vertical displacement. This is the more likely culprit of the increase in altitude seen in the results, due to the fact that the tracking cursor is placed on the end of the projectile that tilted upward. Despite the inherent inaccuracies in the results, Figure 21 does give indication of the flight of the projectile that is confirmed by the still images of the shot seen in Figure 20.
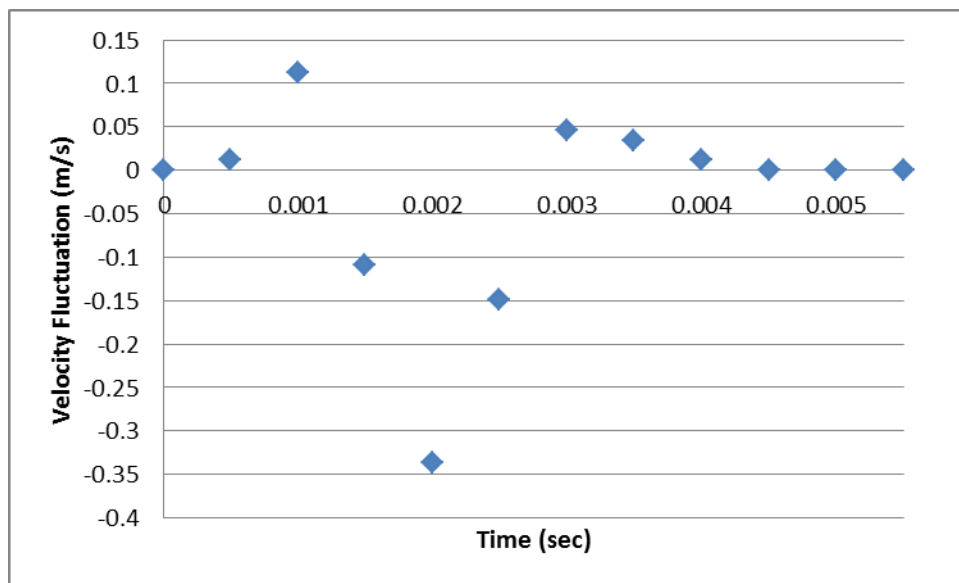

Figure 22: The velocity fluctuation of the projectile with time for the test shot.

The velocity fluctuation of the projectile varies with the flight time as shown in Figure 22. At first, the projectile seems to experience an increase in speed which may be caused by the initial acceleration of the projectile within the barrel. It then experiences a decrease in velocity as the time in flight increases which is typical behavior of projectiles in flight. This behavior seems to disappear, since there is an interval of time when the projectile begins to increase in velocity. This is followed by another period of velocity loss before the results are no longer recorded for the projectile. A possible explanation for the behavior of this projectile may be the tilting of the projectile in flight. The tilting of the projectile may account for the period of lost speed and the following interval of increasing speed may be caused by the flight following the reorientation of the projectile. It is not believed that the method of obtaining the measurements during flight have anything to do with the odd nature of the speed of the projectile. This is because despite the inherent discrepancies in this form of measurement caused by the constant manual retargeting of the tip of the projectile, it should not have prevented an accurate measurement of the speed of the projectile, since the change in position of the tracking point has nothing to do with the overall speed of the projectile in flight. The highest decrease in velocity fluctuation achieved by this projectile was -0.3373 m/s which was achieved 0.002 seconds into the flight. The reason that this speed is negative is that it is below the speed that the projectile achieved in the barrel exit of the gun which is treated as 0 for graphical purposes. The highest increase in velocity fluctuation achieved by the projectile was 0.1131 m/s which occurred 0.001 seconds into flight. The average velocity fluctuation obtained by this projectile was -0.03795 m/s.
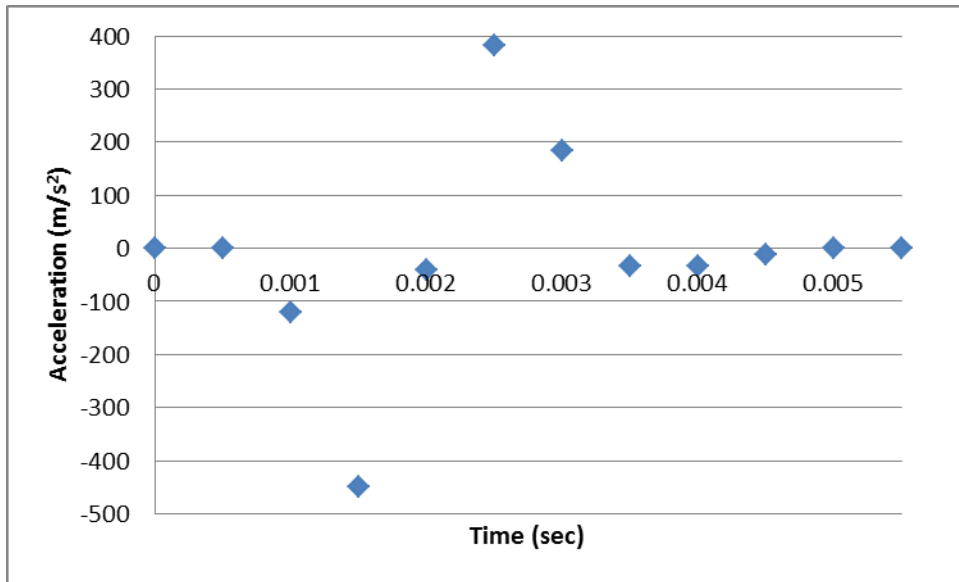
Figure 23: The acceleration of the projectile with time for the test shot.

The acceleration demonstrated by the projectile in flight corresponds to the velocity of the projectile in the time interval recorded, as shown in Figure 23. The data shows a period of deceleration followed by a period of acceleration followed by another period of deceleration. It is believed that since the acceleration of the projectile is related to its velocity, the tilting of the projectile is also responsible for the behavior visible in the data. The greatest amount of deceleration that the projectile experienced was when 0.0015 seconds had passed and was -450.34 m/s^2. Conversely, the greatest amount of acceleration the projectile achieved was 383.29 m/s^2 which was achieved after 0.0025 seconds had passed from the launching of the projectile. The average acceleration obtained by this projectile was -15.57 m/s^2.

4.2 First Shot

The first shot that results were recorded for was fired when the capacitor had reached a power rating of 168.4 volts. The results for this projectile shot were recorded in bits like the

previous shot, but the conversion factor was given as 1 bit = 0.05984 cm due to the fact the shot was recorded over a 25.4 cm span rather a 20.32 cm one.

The average velocity of this shot was 25.4 m/s. The acceleration in the barrel for this shot was calculated to be 5,347.37 m/s^2. The % efficiency of this shot was calculated to be 2.06%.
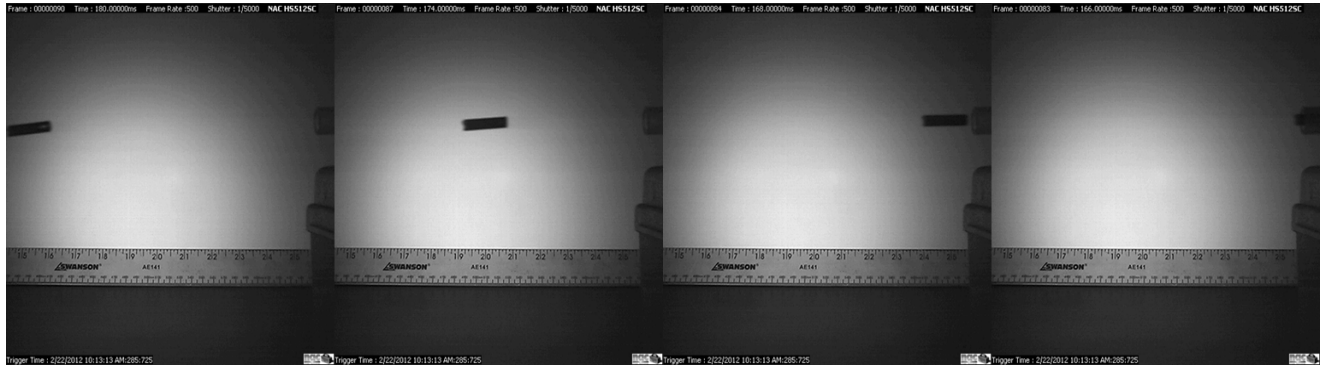

Figure 24: The flight path of the yarn carrier fired at 168.4 volts.

The visual data presented in the still frames of the video of the first shot, shown in Figure 24, does not demonstrate the same phenomenon visible in the previous shot. In this shot, the projectile demonstrates the typical behavior of an object in flight, decreased altitude as distance traveled increased. This suggests that the current within the capacitor has a direct control on the flight path of the projectile.
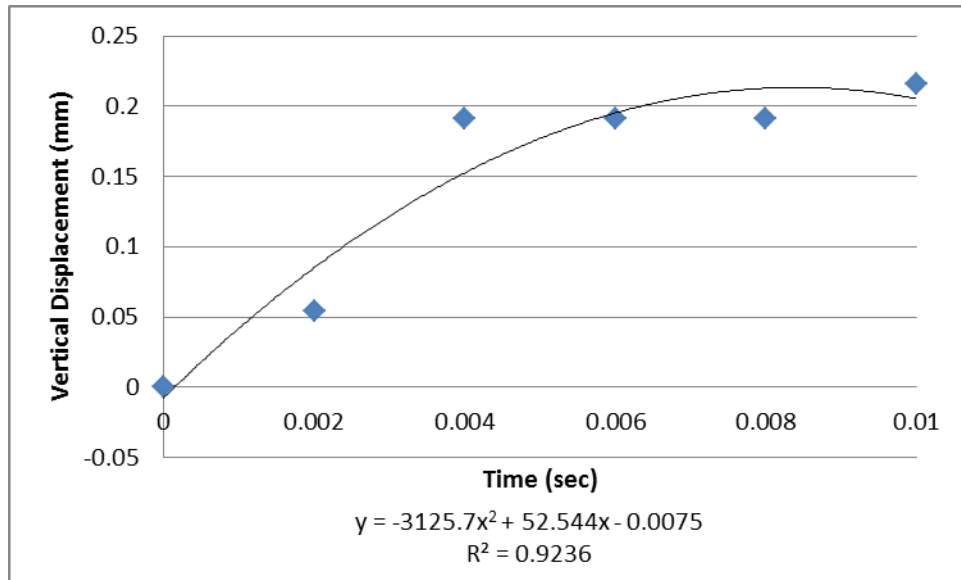
Figure 25: Loss of altitude of the projectile with time for the first shot.

The results for this shot suggest that the projectile gains altitude while in flight and then descends before leveling off and experiencing another brief period of climb, as shown in Figure 25. This conflicts with the visual data that show that the projectile loses altitude over the course of flight. The conflicting results may be the result of air currents since the increase in altitude is negligible. The fall detected is the result of the natural behavior of a projectile in flight and agrees with the evidence provided by the video of the shot. The other brief period of ascent at the end of the flight of the projectile suggests that either the air flow had an effect on the projectile again or that the tracker on the projectile may not have been placed in the same location as before.
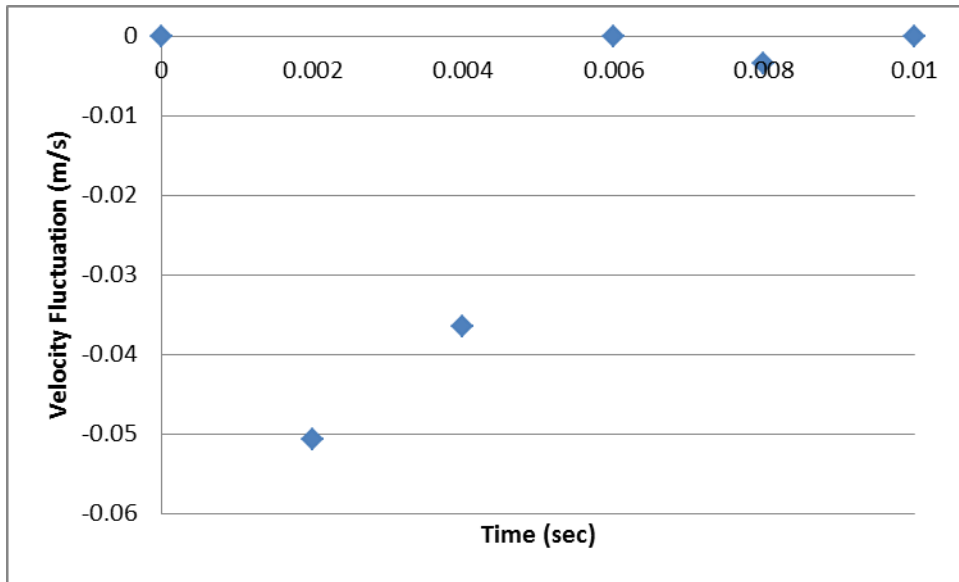
Figure 26: The velocity fluctuation of the projectile with time for the first shot.

The results indicate that the projectile experienced a decrease in speed after it left the barrel of the coil gun, as shown in Figure 26. This immediate loss of speed may be caused by the projectile making additional contact with the inside of the barrel during launch. This may have been caused by the reduced power that the projectile was launched at. After this period of loss of speed, the projectile experiences a phenomenon similar to that shown in the test shot. This projectile did not display any upward tilt in its flight. The highest recorded decrease in velocity fluctuation for this shot occurred at 0.002 seconds into flight and was -0.05066 m/s. The highest recorded increase in velocity fluctuation for this shot was 0 m/s which occurred 0.006 seconds into the flight. This is feasible, since it indicates that the projectile has reached the speed it obtained inside the barrel before exiting. The average velocity fluctuation obtained by this projectile was -0.02269 m/s.
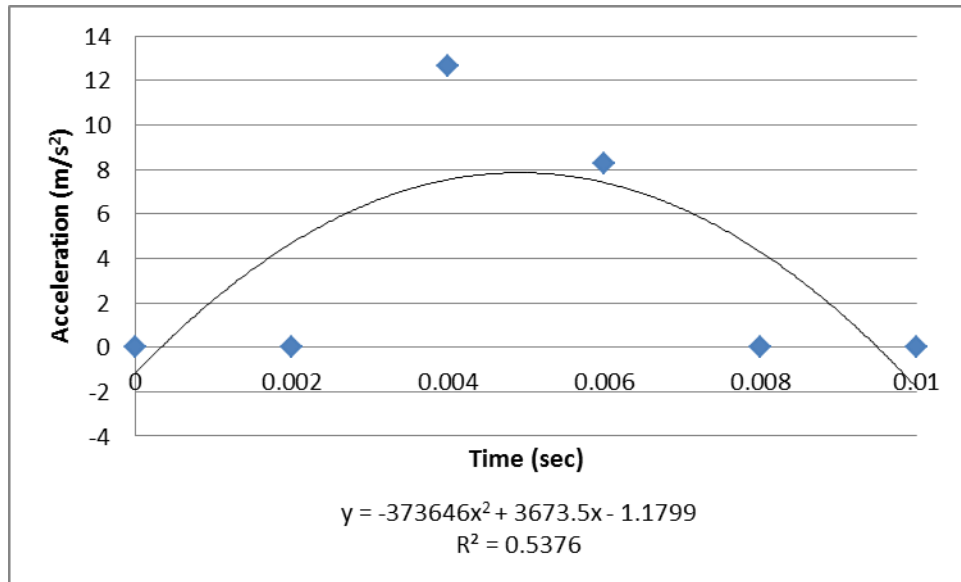
Figure 27: The acceleration of the projectile with time for the first shot.

The results for the acceleration of the projectile as the time in flight increases shows a rise in acceleration, as shown in Figure 27, that corresponds with the increase in speed displayed in the velocity results beginning at the 0.002 second mark. The period of acceleration is the only thing that the results can confirm accurately due to the fact that the projectile managed to "vanish" from the camera's tracking system. The projectile most likely "vanished" because of the way that it had to be tracked. This does not however account for how there is more information gathered about the velocity of the projectile than the acceleration. Due to the projectile "vanishing", the accelerations at that interval of time are recorded as a 0 for graphical purposes. The greatest amount of acceleration the projectile achieved was 12.67 m/s^2 which was accomplished after 0.004 seconds had elapsed since the beginning of its flight. The average acceleration obtained by this projectile was 10.46 m/s^2.

4.3 Second Shot

The second shot that results were recorded for was fired when the capacitor had reached a power rating of 190 volts. The results for this projectile shot were recorded in bits like the test shot, but the conversion factor was given as 1 bit = 0.05962 cm due to the fact the shot was recorded over a 24.89 cm span rather a 25.4 cm one.

The average velocity of this shot was 24.89 m/s. The acceleration in the barrel for this shot was calculated to be 5,134.79 m/s^2. The % efficiency of this shot was calculated to be 1.55%.
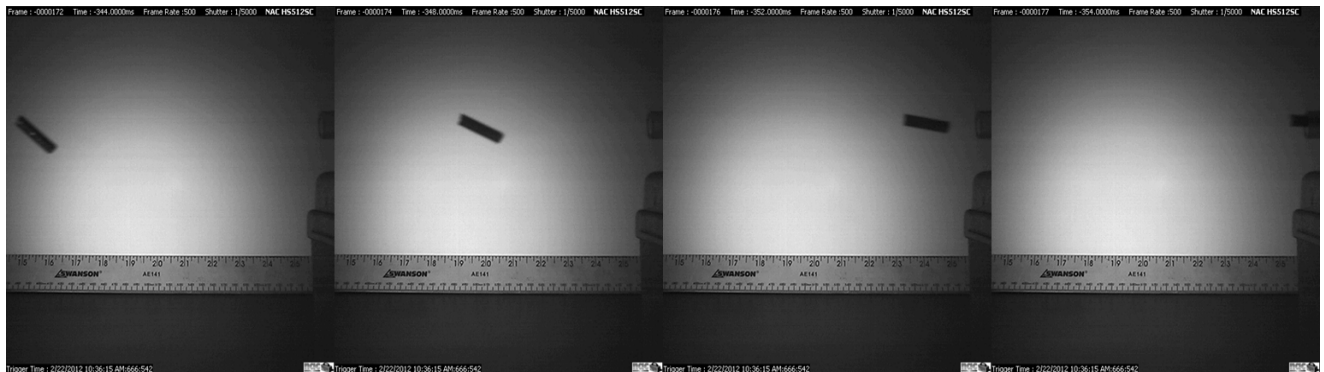

Figure 28: The flight path of the yarn carrier fired at 190 volts.

The visual data presented in the still frames of the video of the second shot, shown in Figure 28, shows that the projectile demonstrates the same phenomenon visible in the test shot. In this shot, the projectile once again tilts upward as it flies while it flies without any loss in altitude. The upward tilt for this projectile is much more pronounced in this shot. This further suggests that the current within the capacitor has a direct control on the flight path of the projectile as well as the tilt of the projectile.
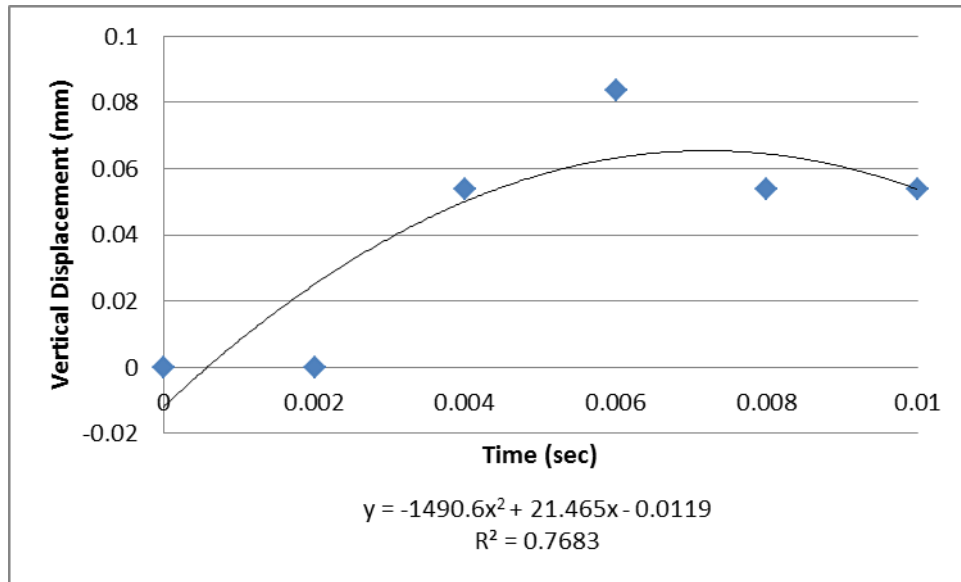
$$y = -1490.6x^2 + 21.465x - 0.0119$$
$$R^2 = 0.7683$$

Figure 29: Loss of altitude of the projectile with time for the second shot.

As shown in Figure 29, the results for the vertical displacement of the projectile fired at 190 volts do not show the typical projectile behavior of losing altitude as the flight time increases until the end of the flight. The increase in altitude indicated by the results is itself the result of the upward tilt of the projectile in flight. The projectile does exhibit expected behavior towards the end of its recorded flight although it does level off and hold a steady altitude. This is supported by the visual evidence provided in the video of the projectile.
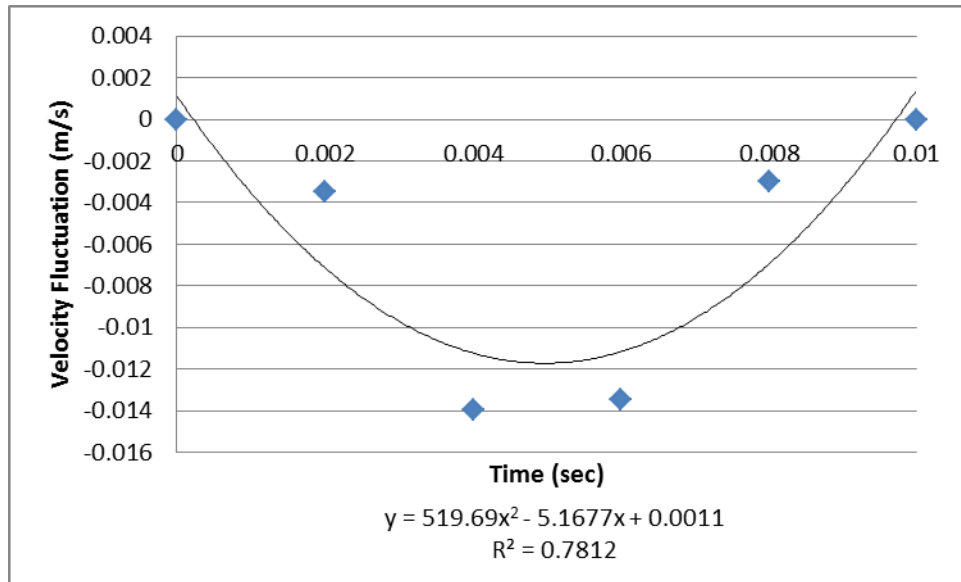
Figure 30: The velocity fluctuation of the projectile with time for the second shot.

As shown in Figure 30, the results of the shot show the same phenomenon that is visible in the previous shots. The projectile begins by showing a decrease in speed after exiting the barrel of the gun. The projectile then begins a period of increasing speed. This could possibly be explained by the tilting of the projectile, since that would allow more surface area for the friction in the air to act on. If this is true, then the increase in velocity may indicate that the projectile overcame the friction in the air after finishing its tilt and regained its lost speed. After the 0.008 second mark, the results become invalid due to the fact that the projectile "vanishes" from the camera's sensor. The highest recorded decrease in velocity fluctuation for this shot was -0.01399 m/s which occurred at 0.004 seconds into the flight. The highest recorded increase in velocity fluctuation for this shot occurred at 0.008 seconds into the flight and was -0.00299 m/s. The average velocity fluctuation that this projectile achieved was -0.00849 m/s.
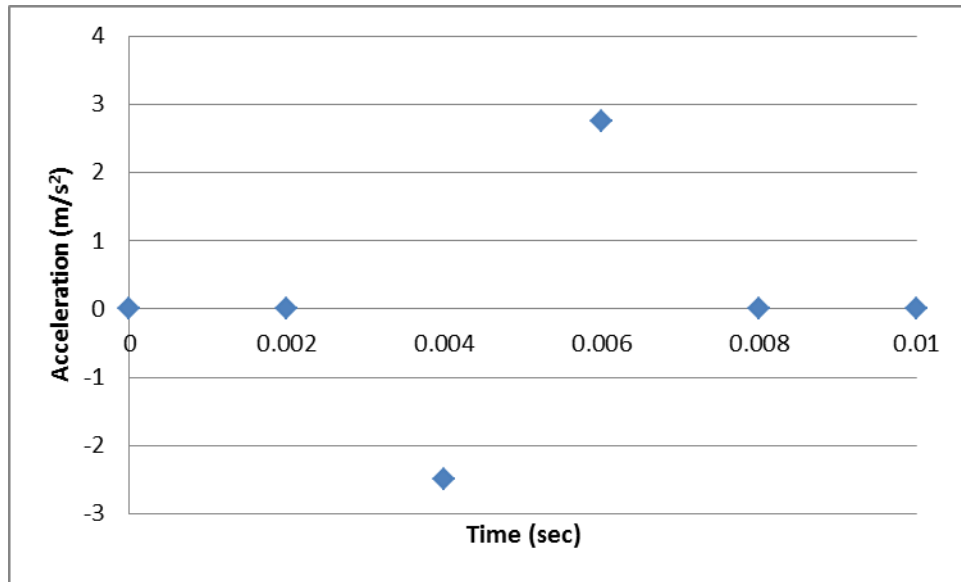
Figure 31: The acceleration of the projectile with time for the second shot.

The results for the acceleration of the projectile, as shown in Figure 31, correspond with the variations in velocity in Figure 30. The peaks are in the graph are the only results that are viable, since once again the projectile "vanished" from camera's sensors for detecting acceleration. Despite this, the results can still be considered accurate due to their correspondence to the results of the velocity tracking. The greatest amount of deceleration that the projectile experienced was when 0.004 seconds had passed and was -2.497 m/s^2. Conversely, the greatest amount of acceleration the projectile achieved was 2.752 m/s^2 which was achieved after 0.006 seconds had passed from the launching of the projectile. This projectile achieved an average acceleration of 0.1278 m/s^2.

4.4 Third Shot

The third shot that results were recorded for was fired when the capacitor had reached a power rating of 170 volts. The results for this projectile shot were recorded in bits like the test

shot, but the conversion factor was given as 1 bit = 0.6015 cm due to the fact the shot was recorded over a 26.67 cm span rather a 25.4 cm one.

The average velocity of this shot was 26.67 m/s. The acceleration in the barrel for this shot was calculated to be 5,895.47 m/s^2. The % efficiency of this shot was calculated to be 2.23%.
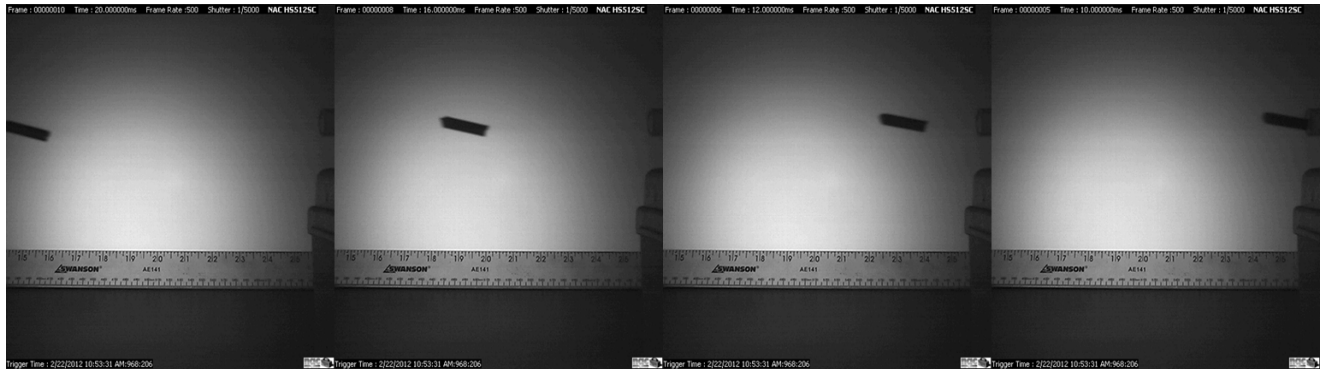

Figure 32: The flight path of the yarn carrier fired at 170 volts.

The visual data presented in the still frames of the video of the third shot, shown in Figure 32, demonstrates the phenomenon visible in the test shot. In this shot, the projectile demonstrates the behavior of an object in flight with a slight upward tilt. This is demonstrated by the fact that as the distance it travels increases its altitude decreases. This adds further evidence to suggest that the current within the capacitor has a direct control on the flight path and tilt of the projectile.
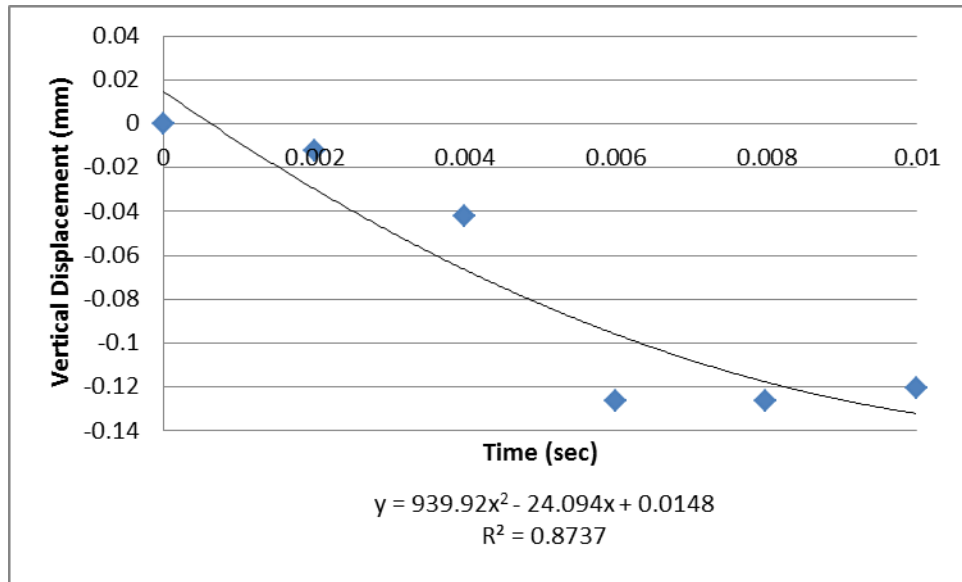
Figure 33: Loss of altitude of the projectile with time for the third shot.

The results for the vertical displacement of the projectile shot at 170 volts, Figure 33, indicate that the projectile experiences typical projectile motion in flight. This is supported by the video and stills of this shot, since they showed the typical projectile behavior of falling in flight as well. It should be noted though that the projectile's flight path appears to have leveled off toward its exit from the camera's view. This indicates that the projectile still had plenty of momentum left to carry it further in flight. The results for this projectile's vertical displacement seem to be the most in tune with what is expected of a projectile.
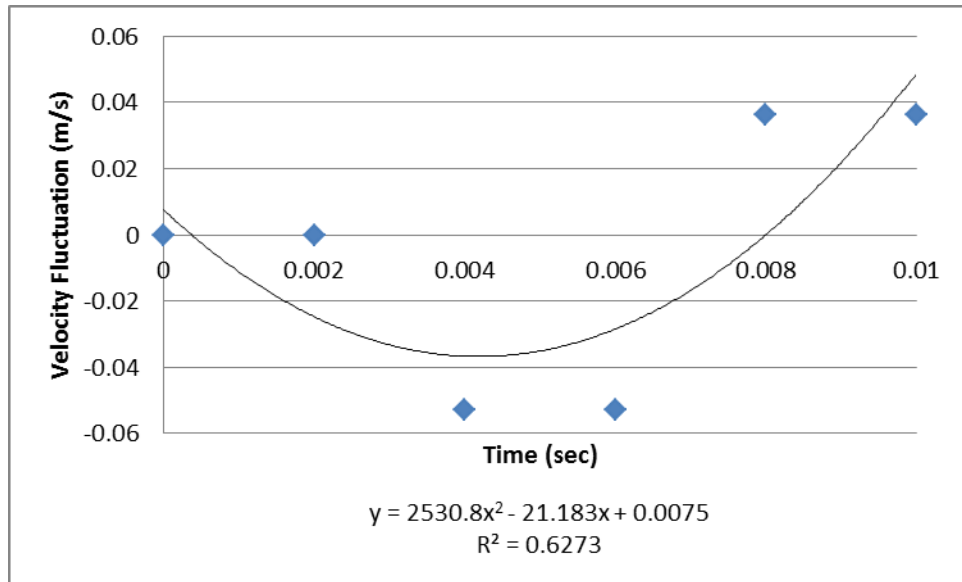
Figure 34: The velocity fluctuation of the projectile with time for the third shot.

As shown in Figure 34, the results for the velocity of the projectile fired at 170 volts show the phenomenon visible in the previous results. The projectile again begins with a period of loss of speed as expected. This is followed by a period of increasing speed that corresponds to the leveling off of the projectile visible in the displacement results. This suggests that the leveling off of the projectile is caused by the increase in the speed of the projectile. The highest recorded decrease in velocity fluctuation for this shot occurred at 0.004 seconds into flight and was maintained until 0.006 seconds into the flight. The highest decrease in velocity fluctuation achieved was -0.05282 m/s. The highest recorded increase in velocity fluctuation for this shot was 0.03609 m/s which occurred at 0.008 seconds into flight and was maintained until 0.010 seconds into the flight. This projectile achieved an average velocity fluctuation of -0.00669 m/s.
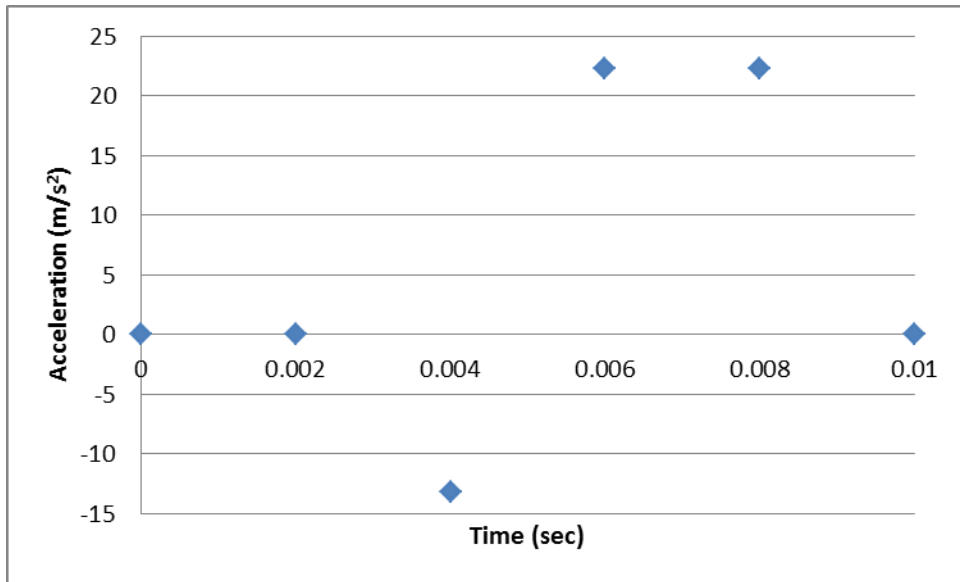
Figure 35: The acceleration of the projectile with time for the third shot.

The acceleration results, shown in Figure 35, correspond to those visible in the results obtained for the velocity. The peak periods of acceleration and deceleration are again the only results on the graph that are accurate. This is because the projectile once again "vanished" from the camera's acceleration sensors. The greatest amount of deceleration that the projectile experienced was when 0.004 seconds had passed and was -13.20 m/s^2. Conversely, the greatest amount of acceleration the projectile achieved was 22.23 m/s^2 which was achieved after 0.006 seconds had passed and maintained until 0.008 seconds had passed from the launching of the projectile. This projectile achieved an average acceleration of 10.42 m/s^2.

4.5 Fourth Shot

The fourth shot that results were recorded for was fired when the capacitor had reached a power rating of 199 volts. The results for this projectile shot were recorded in bits like the test

shot, but the conversion factor was given as 1 bit = 0.05976 cm due to the fact the shot was recorded over a 25.15 cm span rather a 26.67 cm one.

The average velocity of this shot was 25.15 m/s. The acceleration in the barrel for this shot was calculated to be 5,242.62 m/s^2. The % efficiency of this shot was calculated to be 1.45%.
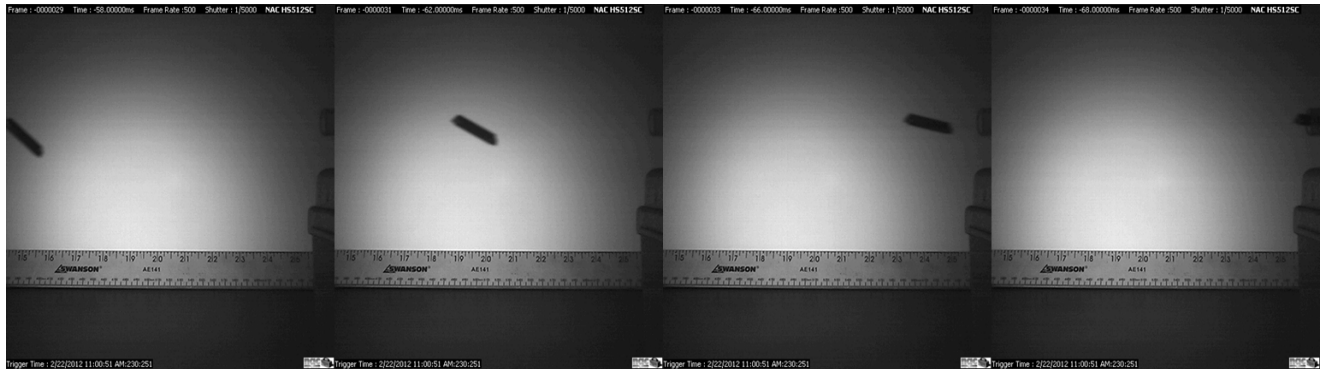

Figure 36: The flight path of the yarn carrier fired at 199 volts.

The visual data presented in the still frames of the video of the fourth shot, shown in Figure 36, demonstrates the same phenomenon visible in the test shot and the second shot. In this shot, the projectile tilts upward at an even greater degree than that of the previous projectiles that displayed this phenomenon. This projectile flies straight over the distance covered in the test with the only variation in flight being the extreme upward tilt. This continues to suggest that the current within the capacitor has a direct control on the flight path and tilt of the projectile.
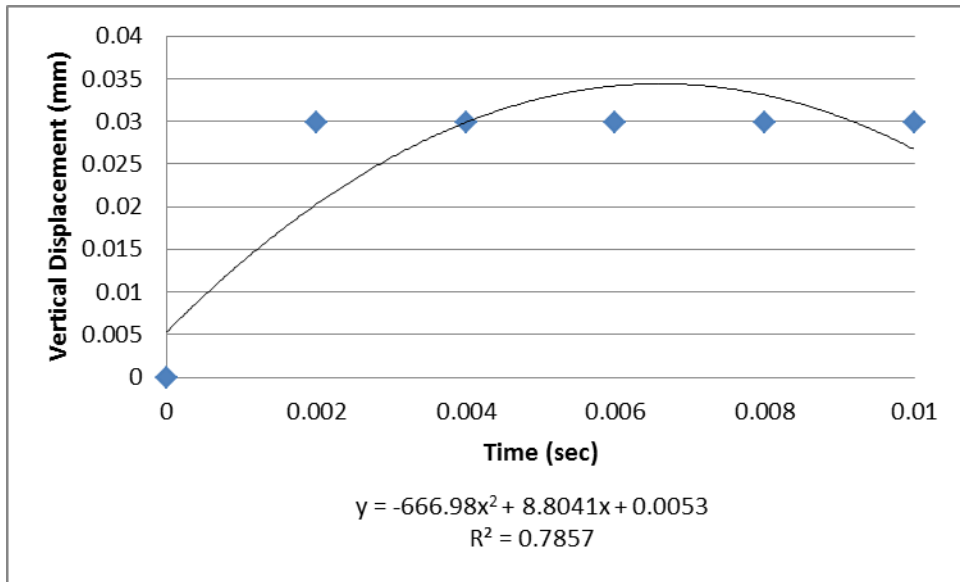
Figure 37: Loss of altitude of the projectile with time for the fourth shot.

The results for the shot at 199 volts, shown in Figure 37, show what appears to be a rapid increase in altitude. This is only visible during the initial stages of the projectile's flight path before eventually leveling off and maintaining a constant altitude. This projectile experienced the most severe amount of tilt during flight of any of the projectiles. This means that the rise in altitude at the beginning of its flight is the direct result of the tilting of the projectile. The results also show that after the initial period of tilting, the projectile flies extremely straight for the rest of the recorded interval.
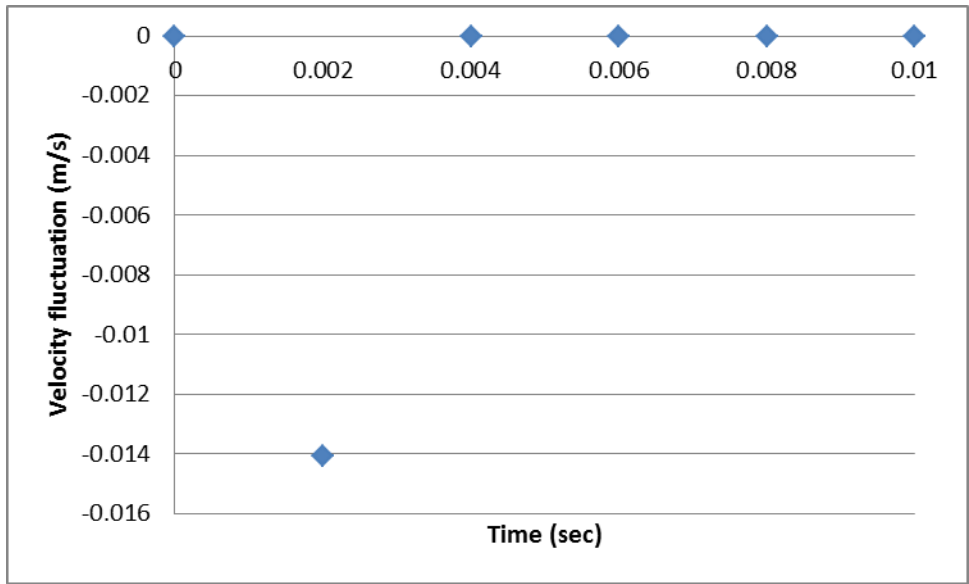
Figure 38: The velocity fluctuation of the projectile with time for the fourth shot.

The results for the velocity of the shot at 199 volts, shown in Figure 38, demonstrate the velocity phenomenon that has been visible in the results of the previous shots. The loss of velocity shown in the beginning of this shot suggests typical projectile behavior. In actuality though, the decrease in velocity at the beginning of the projectile's recorded flight is more than likely the result of the extreme tilting of the projectile giving air resistance a greater surface area to work on. This means that the subsequent increase in velocity is the result of the projectile overcoming the air resistance and holding a steady flight path. The highest recorded decrease in velocity fluctuation for this projectile is -0.01406 m/s which occurred 0.002 seconds into its flight. The highest recorded increase in velocity fluctuation for this shot was 0 m/s which occurred 0.004 seconds into the flight and was maintained throughout the rest of its recorded flight. This indicates that the projectile once again achieved the velocity it had inside the barrel. The average velocity fluctuation of this projectile was -0.00352 m/s.
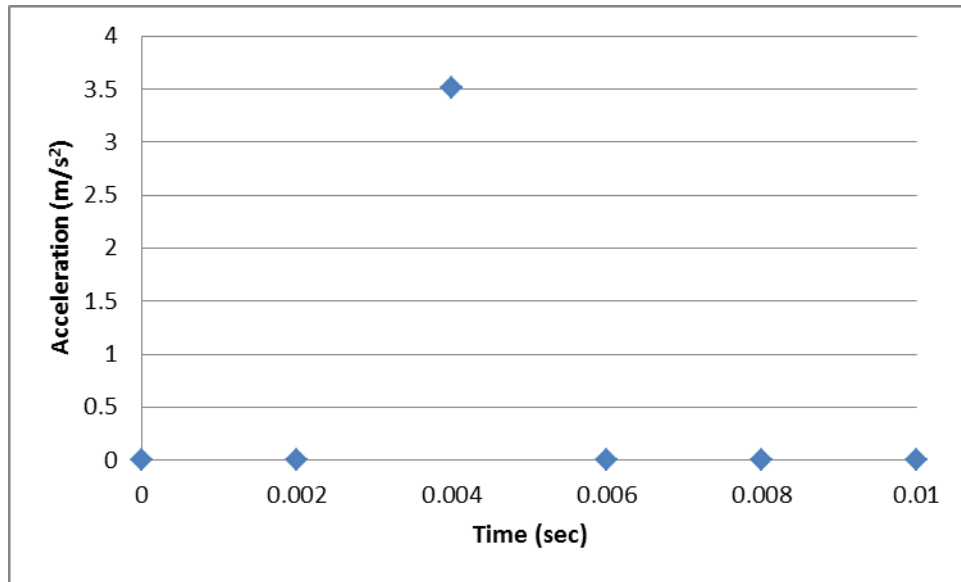
Figure 39: The acceleration of the projectile with time for the fourth shot.

As show in Figure 39, the acceleration results actually do not account for the period of velocity loss at the beginning of the flight. This is because the projectile once again "vanished" from the camera's acceleration sensors. The results do accurately represent the period of increasing velocity visible in Figure 38. This is followed by a drop in acceleration that should have leveled off like the velocity had the camera not lost track of the projectile again after 0.006 seconds had elapsed in its flight time. The highest amount of acceleration that the projectile achieved was after 0.004 seconds had passed in its flight and was recorded as 3.515 m/s^2. The lowest amount of acceleration that was recorded was 0 m/s^2 which was after 0.006 seconds had passed in flight. This corresponds to the constant velocity experienced at the end of the projectile's recorded flight. The average acceleration of this projectile was 1.758 m/s^2.

4.6 Fifth Shot

The fifth shot that results were recorded for was fired when the capacitor had reached a

power rating of 196 volts. The results for this projectile shot were recorded in bits like the test

shot, but the conversion factor was given as 1 bit = 0.05962 cm due to the fact the shot was

recorded over a 24.89 cm span rather a 25.15 cm one.

The average velocity of the projectile was 31.12 m/s. The acceleration in the barrel for

this shot was calculated to be 8026.97 m/s^2. The % efficiency of this shot was calculated to be
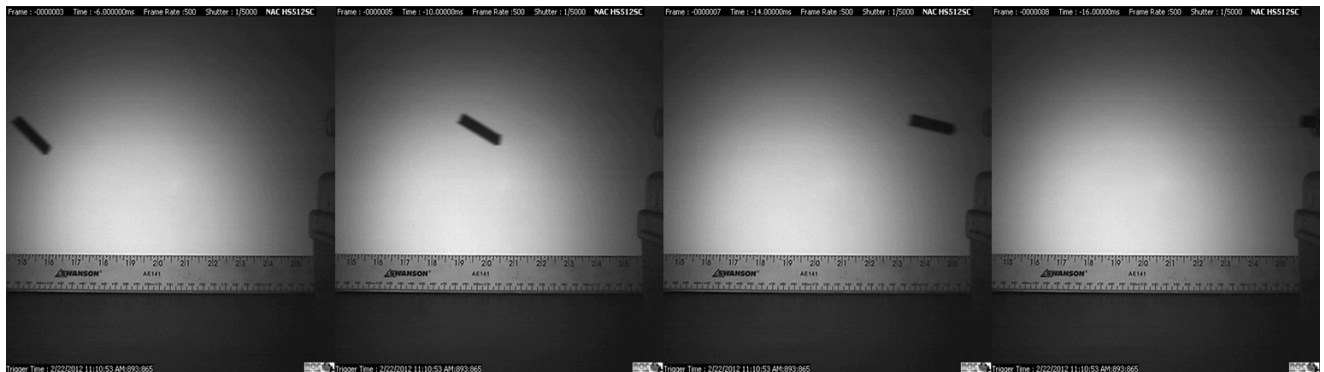
2.28%.

Figure 40: The flight path of the yarn carrier fired at 196 volts.

The visual data presented in the still frames of the video of the fifth shot, shown in Figure

40, demonstrate the same phenomenon visible in the test shot. In this shot, the projectile tilts

upward as it flies, but otherwise remains straight in flight. It is notable in this shot that despite

the fact that only 3 volts separate this shot from the last, that the tilt of the projectile is noticeably

not as great. This lends further credibility to the theory that the current within the capacitor has a

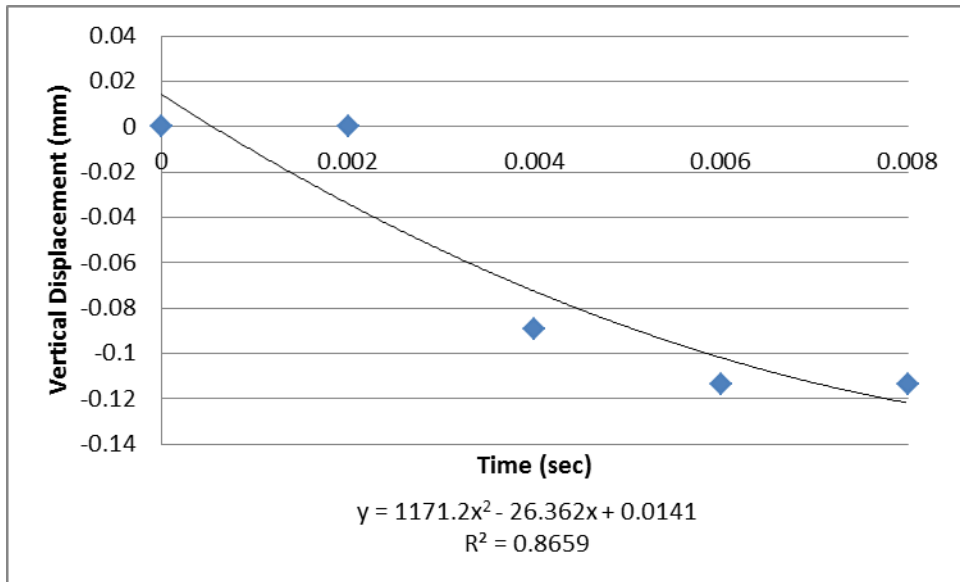direct control on the flight path and tilt of the projectile.

Figure 41: Loss of altitude of the projectile with time for the fifth shot.

The results for the vertical displacement of the projectile shot at 196 volts, shown in Figure 41, do not seem to follow the trend of the projectiles that tilt in flight. They do, however, display expected projectile behavior. The results were expected to be similar to those obtained from the shot at 199 volts due to the large tilt visible in both shots, Figure 36 and 40. In fact, the exact opposite occurred in the flight of this projectile with the eventual leveling off included, causing a conflict between the visual and graphical results. It should be noted that the results for this shot only cover a 0.008 second interval rather than a 0.01 second interval like the previous ones. This is because the projectile "vanished" from the camera's displacement sensors around this time, something not experienced in the previous shots.
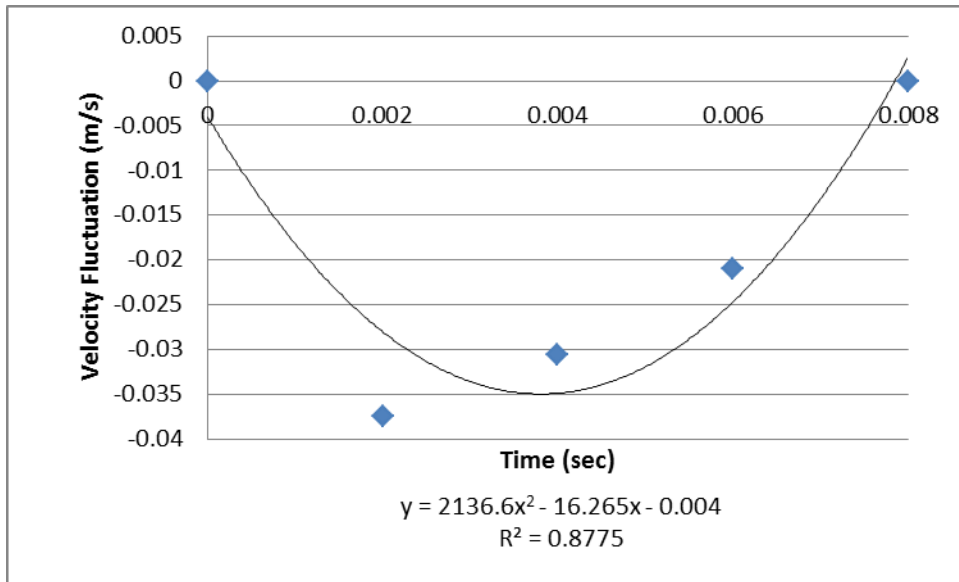
Figure 42: The velocity fluctuation of the projectile with time for the fifth shot.

The velocity results for this shot, Figure 42, indicate the same phenomenon visible in the previous shots. The results depict a loss in speed which probably corresponds to the tilting of the projectile followed by a rise in speed. The highest recorded decrease in velocity for this shot was -0.03755 m/s which occurred after 0.002 seconds. The highest recorded increase in velocity was achieved 0.006 seconds into the flight and was -0.0210 m/s. The average velocity fluctuation of this projectile was -0.0297 m/s.
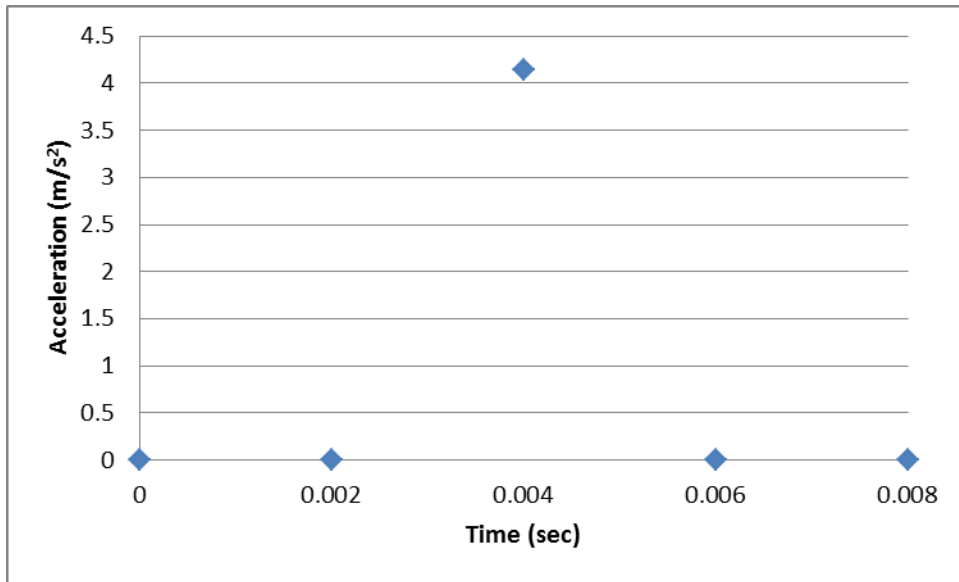
Figure 43: The acceleration of the projectile with time for the fifth shot.

The acceleration results for this shot, Figure 43, depict a period of acceleration that is confirmed in the velocity results, Figure 42. Unfortunately, this is the only accurate reading on the graph due to the camera being unable to keep track of the projectile for acceleration aside for the 0.004 second mark. The results for the acceleration of this projectile are not very viable due to this fact. The only recorded acceleration for this projectile occurred at the 0.004 second mark and was 4.139 m/s^2.

4.7 Sixth Shot

The sixth shot that results were recorded for was fired when the capacitor had reached a power rating of 185 volts. The results for this projectile shot were recorded in bits like the previous shot, but the conversion factor was given as 1 bit = 0.06681 cm due to the fact the shot was recorded over a 22.86 cm span rather a 25.4 cm one.

The average velocity of this projectile was 19.05 m/s. The acceleration in the barrel for this shot was calculated to be 3007.89 m/s^2. The % efficiency of this shot was calculated to be 0.96%.
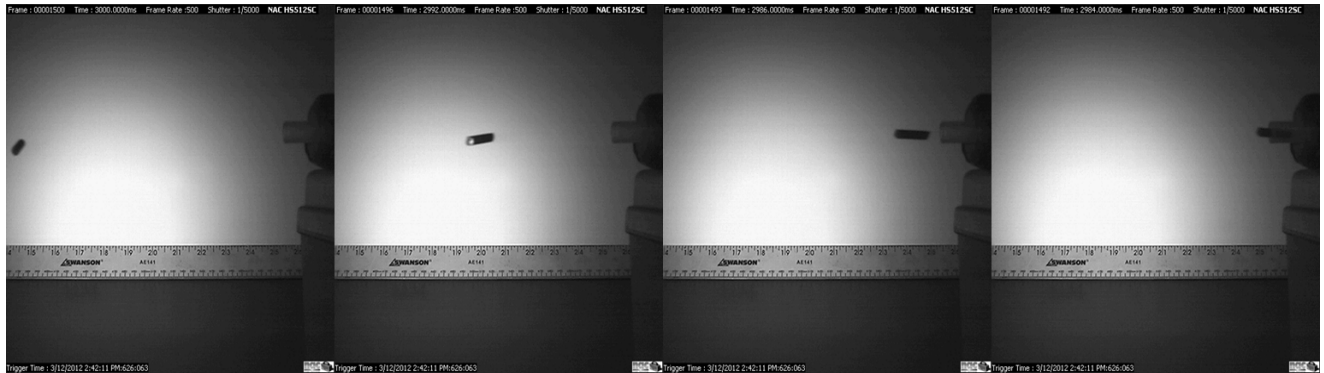

Figure 44: The flight path of the yarn carrier fired at 185 volts that rotated 90 degrees in mid-air.

The visual data for this shot, shown in Figure 44, shows a phenomenon that is not visible in any of the previous shots. The projectile appears to rotate 90 degrees left in mid-air. The rotation may have been caused by air resistance though this was not a problem for any of the previous shots. The rotation of this projectile would be a non-issue if it were launched within the reed of a weaving machine to help guide its flight. Although the projectile experiences a rotation, there is little visible descent in flight other than towards the end of the projectile flight. It is notable that this projectile has little upward tilt during its flight similar to what was visible in the test shot which was launched around the same voltage. This adds further evidence to the theory that the power of the capacitor at the time of the shot has direct control over the tilt and flight path of the projectile.
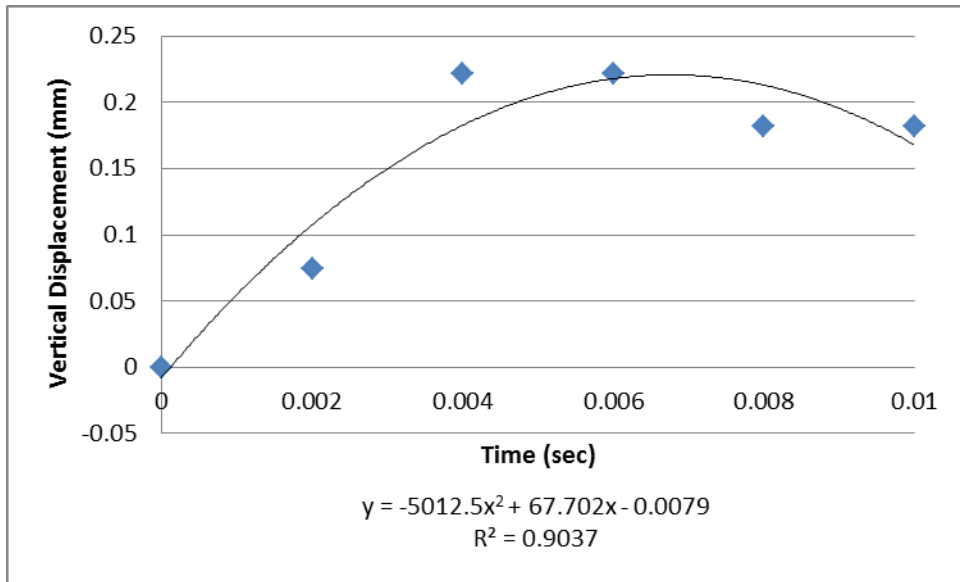
Figure 45: Loss of altitude of the projectile with time for the sixth shot.

The results for the vertical displacement of this projectile shot at 185 volts, shown in

Figure 45, show an interesting behavior: a rise in altitude. This is interesting in the fact that there

is little upward tilt visible in the projectile though this could be attributed to the air resistance

that later caused the projectile to rotate in mid-flight. After the initial period of altitude gain, the

projectile begins to show typical projectile behavior by losing altitude corresponding to the time

in flight. It should be noted that the results indicate that the projectile levels out toward the end

of its recorded flight indicating that it still had plenty distance left to fly.
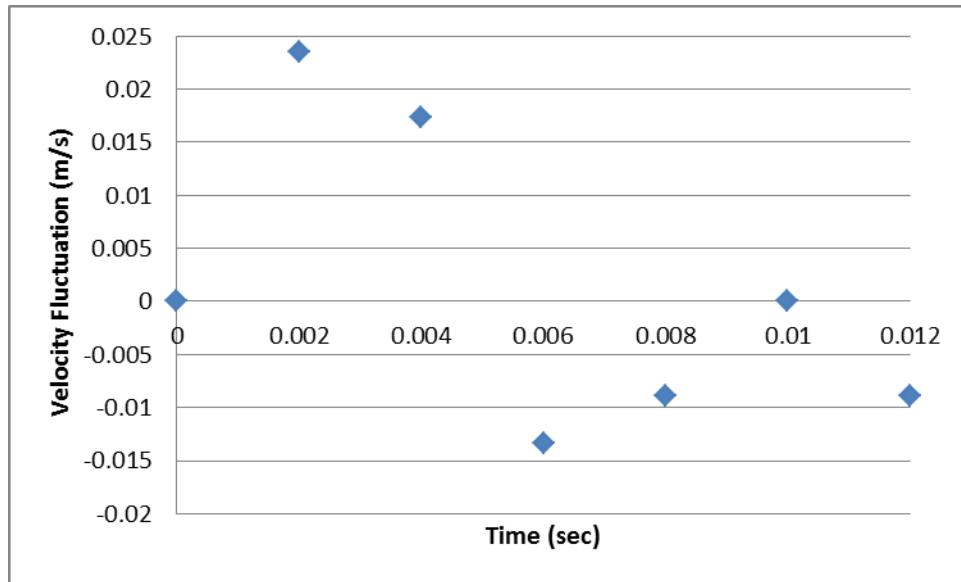
Figure 46: The velocity fluctuation of the projectile with time for the sixth shot.

The results for the velocity fluctuation of the shot at 185 volts, shown in Figure 46, show a similar behavior to previous shots. The projectile gains velocity as it exits the barrel of the gun. This is followed by a period of velocity loss which probably due to air resistance. The negative peak in the velocity results is probably directly caused by the projectile rotating in mid-air which provided a much greater surface area for the air resistance to spread over. The following increase in speed is probably the result of the projectile's velocity overcoming the air resistance and returning to its speed within the barrel. The results for this projectile carry on for another 0.002 seconds further than the other projectiles due to it not "vanishing" from the camera. This additional time shows that the projectile once again began to lose velocity after regaining the speed it had within the barrel. The maximum increase in velocity fluctuation of this projectile was reached 0.002 seconds into its flight and was 0.02347 m/s. The greatest loss in velocity fluctuation that this projectile achieved was 0.006 seconds into its flight and was -0.01335 m/s. The average velocity fluctuation of this projectile was 0.00372m/s.
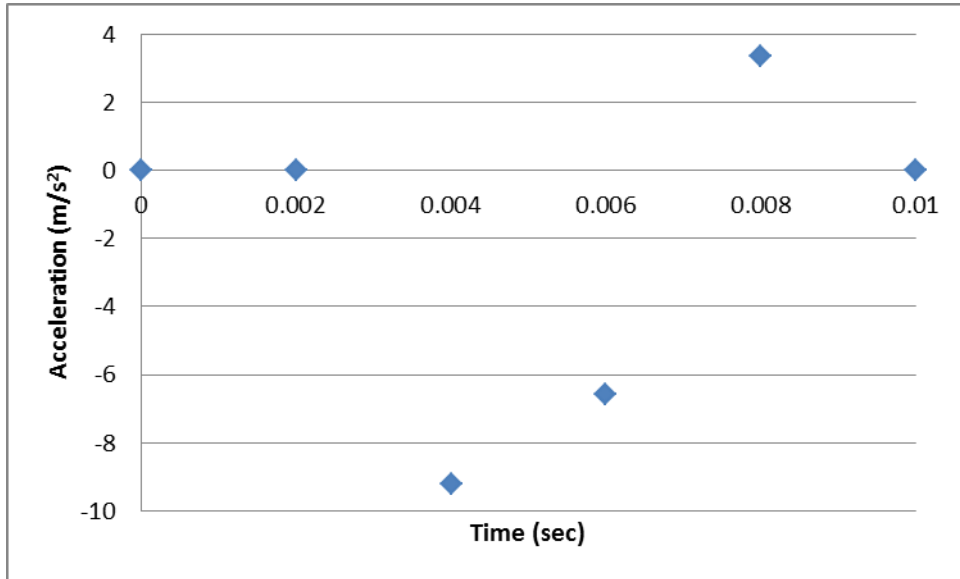
Figure 47: The acceleration of the projectile with time for the sixth shot.

The results for the acceleration of the projectile launched at 185 volts, shown in Figure 47, do not match up with the velocity results in some places. This is a direct result of the projectile "vanishing" from the camera's acceleration sensors for the first 0.002 seconds of its recorded flight. The rest of the results match up well with the velocity results. This includes the large amount of deceleration experienced while the projectile was rotating in mid-air. The period of acceleration afterwards also matches with the velocity results. The deceleration that occurs after the 0.01 second mark is partially visible in the final section of the results though the projectile once again "vanished" at 0.012 second mark and was therefore not included on the graph. The maximum acceleration recorded for the projectile was achieved 0.008 seconds into its flight and was 3.337 m/s^2. The greatest deceleration the projectile experienced was 0.004 seconds into its flight during the turn and was -9.206 m/s^2. The average acceleration of this projectile was -3.109 m/s^2.

4.8 Seventh Shot

The seventh shot that results were recorded for was fired when the capacitor had reached a power rating of 180 volts. The results for this projectile shot were recorded in bits like the previous shot, but the conversion factor was given as 1 bit = 0.06706 cm due to the fact the shot was recorded over a 24.13 cm span rather a 22.86 cm one.

The average velocity of this projectile was 24.13 m/s. The acceleration in the barrel for this shot was calculated to be 4826 m/s^2. The % efficiency of this shot was calculated to be 1.63%.

Figure 48: The flight path of the yarn carrier fired at 180 volts.

The visual data for the projectile fired at 180 volts, shown in Figure 48, demonstrates a phenomenon that seems in direct opposition to the upward tilt that other projectiles have experienced. In the stills of the video, the projectile seems to experience a slight downward tilt throughout its flight. Other than this occurrence, the projectile experiences a visually straight flight path. It also begins to demonstrate typical projectile behavior toward the end of its recorded flight when it descends slightly.
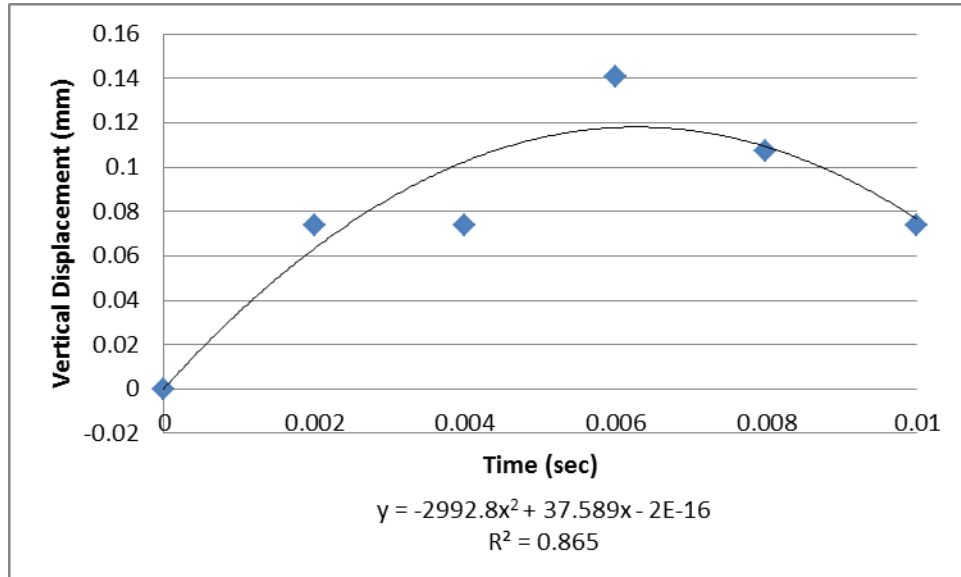
Figure 49: Loss of altitude of the projectile with time for the seventh shot.

The results for the vertical displacement of the projectile shot at 180 volts, shown in Figure 49, demonstrate a similar phenomenon as the previous shots. The projectile appears to experience a period of altitude gain followed by a slight drop in altitude. This is followed by another climb in altitude which is followed by a greater period of loss of altitude that continues until the end of its recorded flight. The rise in altitude is more than likely the result of air resistance once again. It is interesting to note that the amount of altitude increased at much as it did considering that the projectile also tilted slightly downward. Also of note is that this projectile appears to experience two periods of typical projectile behavior.
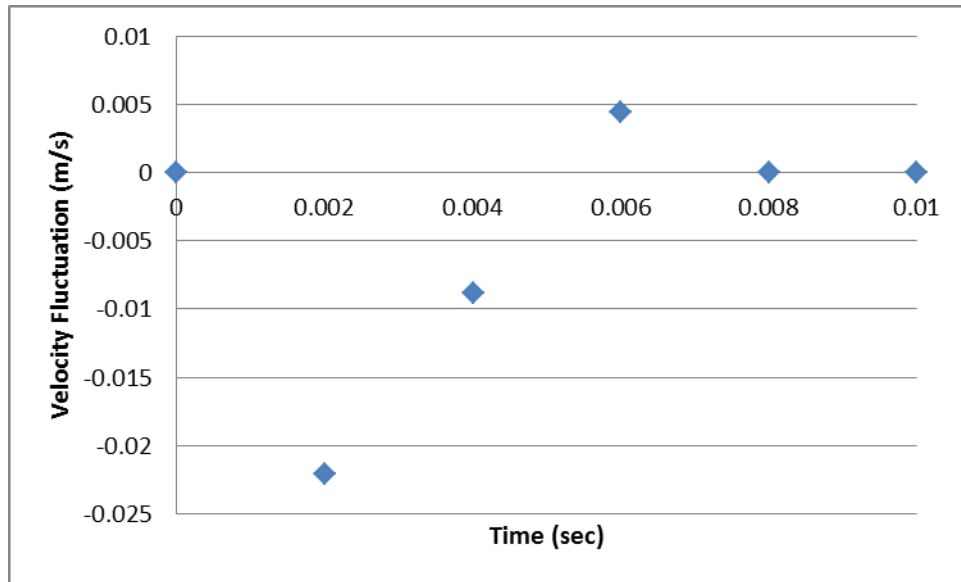
Figure 50: The velocity fluctuation of the projectile with time for the seventh shot.

The results for the velocity fluctuation of the projectile shot at 180 volts, Figure 50, demonstrate similar behavior to some of the previous shots. The projectile experiences a period of deceleration at the beginning of its flight. This is caused by the air resistance combined with the downward tilt of the projectile producing drag. Once this projectile adjusts to this drag, it increases in velocity until reaching a peak. What follows is a slight period of loss of velocity until it returns to the velocity achieved inside the barrel of the gun. The highest decrease in velocity fluctuation that the projectile achieved was -0.02212 m/s. This was obtained 0.002 seconds into its flight. The highest change in velocity fluctuation of the projectile occurred 0.006 seconds into its flight and was 0.00443 m/s. The average velocity fluctuation of this projectile was -0.00531 m/s.
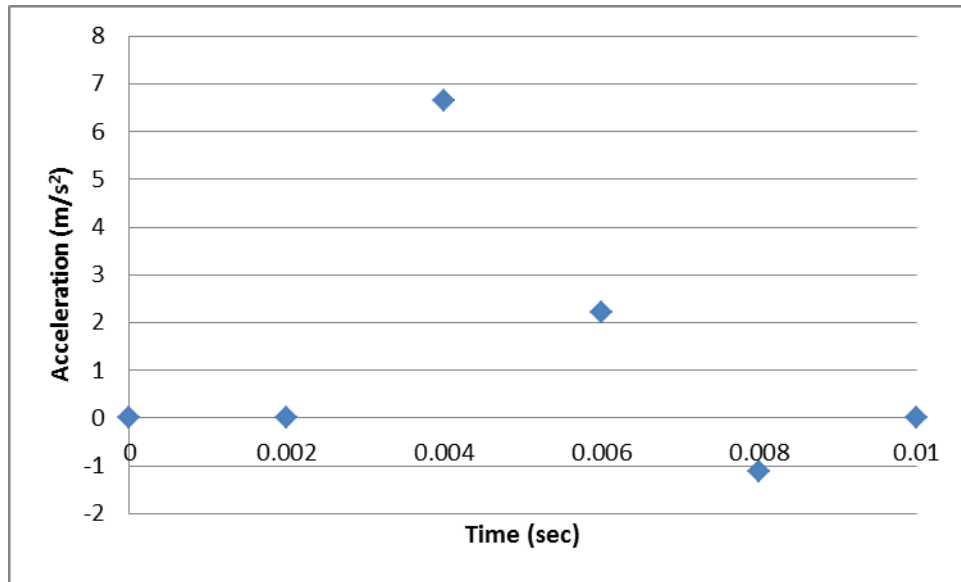
Figure 51: The acceleration of the projectile with time for the seventh shot.

The results for the acceleration of the projectile fired at 180 volts, Figure 51, do not exactly match up with the velocity results. This is because when the initial decrease in velocity is occurring, the projectile had "vanished" from the camera's acceleration sensor. The first results recorded for the acceleration occur at the 0.004 second mark at which point the projectile had achieved a peak in acceleration. The results then continue to correspond to the velocity results experiencing a period of deceleration until the 0.01 second mark at which point the projectile "vanished" again. The highest amount of acceleration achieved by this projectile was 6.635 m/s^2 which occurred at the 0.004 second mark. The greatest amount of deceleration achieved by this projectile was -1.106 m/s^2 which occurred at the 0.008 second mark. The average acceleration achieved by this projectile was 2.580 m/s^2.

4.9 Eighth Shot

The eighth official shot that results were recorded for was fired when the capacitor had reached a power rating of 185 volts again in order to see if the mid-air turn happened again. This power level was repeated due to the midair turning that the previous shot at 185 volts experienced in flight. The results for this projectile shot were recorded in bits like the previous shot, but the conversion factor was given as 1 bit = .06731 cm due to the fact the shot was recorded over a 24.38 cm span rather a 24.13 cm one.

The average velocity of this projectile was 24.38 m/s. The acceleration in the barrel for this shot was calculated to be 4926.52 m/s^2. The % efficiency of this shot was calculated to be 1.57%.

Figure 52: The flight path of the yarn carrier fired at 185 volts that flew straight.

The visual data for the projectile shot at 185 volts, shown in Figure 52, does not show the same mid-air turn that occurred in the previous shot at 185 volts. This shot does however demonstrate the same slight downward tilt that was visible in the shot at 180 volts. The projectile follows a visually straight flight path at this power level. There does not appear to be any loss in altitude visually. It is unknown why the previous shot at 185 volts showed a mid-air 90 degree

rotation but this one did not, since both were fired under the same conditions unless the air flow was somehow different in the room.
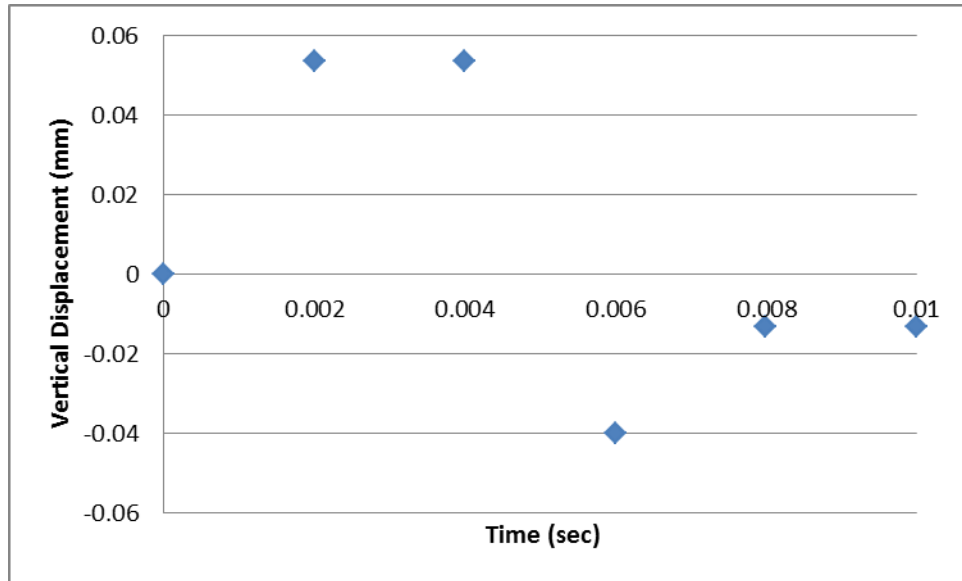

Figure 53: Loss of altitude of the projectile with time for the eighth shot.

The vertical displacement results for the second projectile shot at 185 volts, shown in Figure 53, indicate that air currents greatly affected the altitude of this projectile. This is first made evident during the initial stages of the projectile's recorded flight when an increase in altitude is recorded. This period of increasing altitude is followed by a period of decreasing altitude that is typical of normal projectile behavior. Another period of increasing altitude follows which is again probably the result of air currents. The projectile then levels off and maintains a steady altitude during the end of its recorded flight.
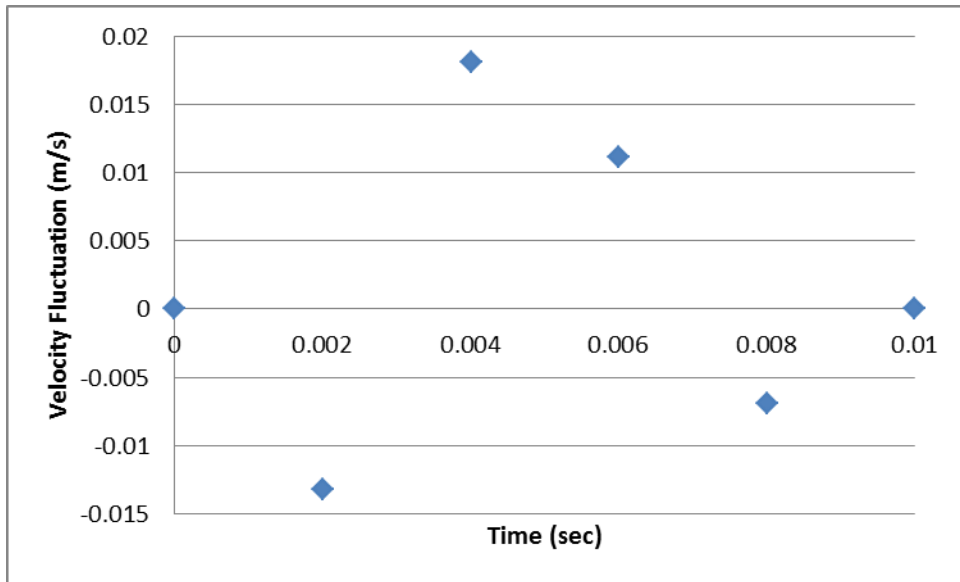
Figure 54: The velocity fluctuation of the projectile with time for the eighth shot.

The velocity results for the second projectile fired at 185 volts, Figure 54, show a similar trend that is visible in the previous shots. The projectile starts by losing velocity at the beginning of its flight. This is followed by a period of increasing velocity until a peak is achieved. After the peak was reached the projectile once again goes through a period of decreasing velocity. The graphical results indicate another period of increasing velocity towards the end of its recorded flight. This is not the case though since the projectile "vanishes" from the camera's velocity tracker with the resulting increase in velocity being the effect of a zero into the results for graphical purposes. The maximum increase in velocity fluctuation achieved by this projectile was 0.01813 m/s which was achieved 0.004 seconds into its flight. The highest decrease in velocity fluctuation the projectile achieved was -0.01319 m/s which was achieved 0.002 seconds into its flight. The average velocity fluctuation of this projectile was 0.00228 m/s.
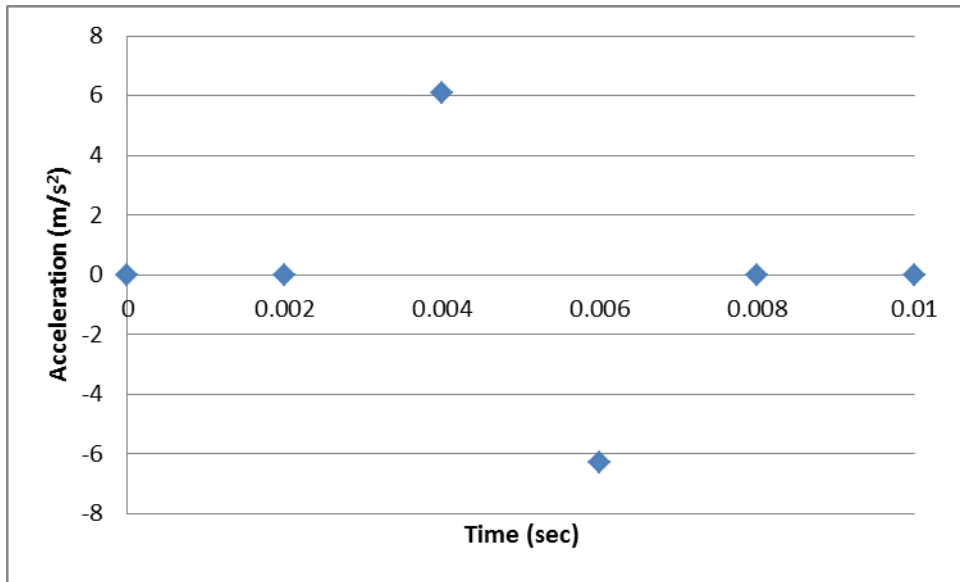
Figure 55: The acceleration of the projectile with time for the eighth shot

The acceleration results for the second projectile fired at 185 volts, Figure 55, once again do not exactly match up with the velocity results. This is caused by the fact that during the first 0.002 seconds of the projectile's flight, the projectile "vanishes" from the view of the camera's acceleration tracker. This causes the initial loss of velocity the projectile experiences to not be reflected by a period of deceleration in the acceleration results. Despite this rough start, the results begin to match up with the velocity results after the 0.002 second mark reaching a peak acceleration of 6.087988 m/s^2 at 0.004 seconds which corresponds with the peak velocity achieved by the projectile. This is followed by a period of deceleration that reaches a peak of -6.27295 m/s^2 at 0.006 seconds which corresponds to the period of decreasing velocity. The results after the 0.006 second mark are also inaccurate as the projectile "vanishes" again. The average acceleration achieved by this projectile was -0.09248 m/s^2.

4.10 Ninth Shot

The ninth official shot that results were recorded for was fired when the capacitor had

reached a power rating of 175 volts. The results for this projectile shot were recorded in bits like

the previous shot, but the conversion factor was given as 1 bit = 0.0668 cm due to the fact the

shot was recorded over a 22.86 cm span rather than a 24.38 cm one.

The average velocity of this projectile was 22.86 m/s. The acceleration in the barrel for

this shot was calculated to be 4331.37 m/s^2. The % efficiency of this shot was calculated to be
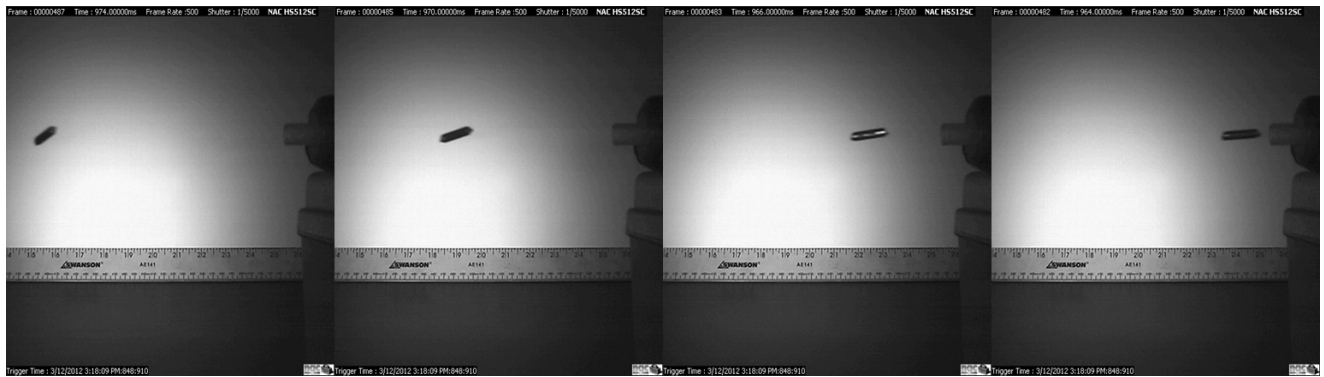
1.54%.

Figure 56: The flight path of the yarn carrier fired at 175 volts.

The visual data for the projectile fired at 175 volts, Figure 56, demonstrate a similar flight

path to the shots fired at 180 and 185 volts. This is because there is a slight downward tilt seen in

the projectile's flight. This is must be the result of air currents affecting the flight path of the

projectile. The projectile also experiences a 90 degree mid-air rotation towards the end of its

recorded flight like the first projectile fired at 185 volts. This is more than likely the result of air

currents again. Despite the fact that it rotated in mid-air, the projectile maintains a visually
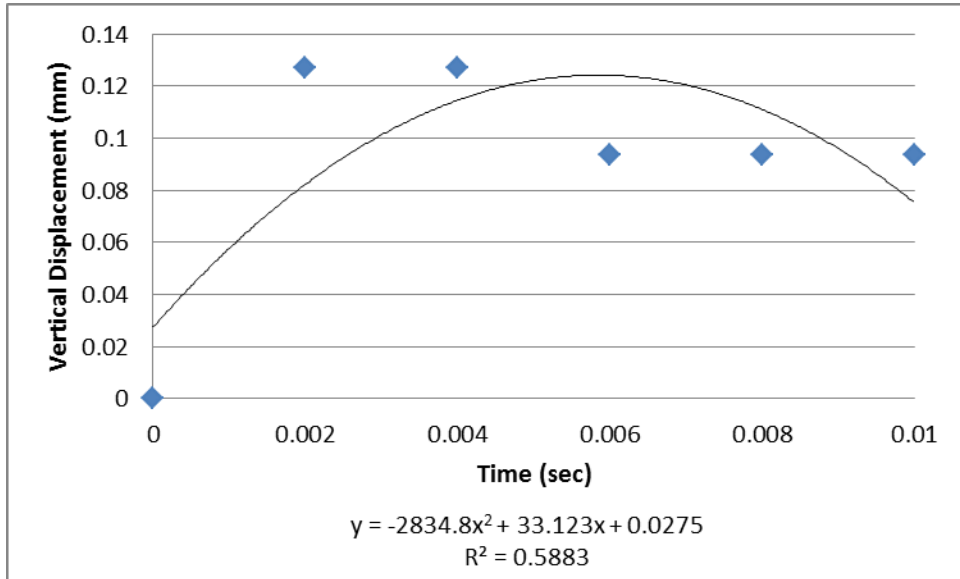
straight flight path.

Figure 57: Loss of altitude of the projectile with time for the ninth shot.

The vertical displacement results for the projectile shot at 175 volts, Figure 57, show behavior that was seen in some of the previous shots. At first, the projectile experiences a period of gaining altitude. After the period of rising altitude, the projectile experiences a brief interval of loss of altitude over a 0.002 second period of time. Following the loss of altitude, the projectile levels off and maintains its altitude through the rest of its recorded flight. It should be noted that the projectile was going through its mid-air rotation during this period of level flight. These results appear to match up with the visual data.
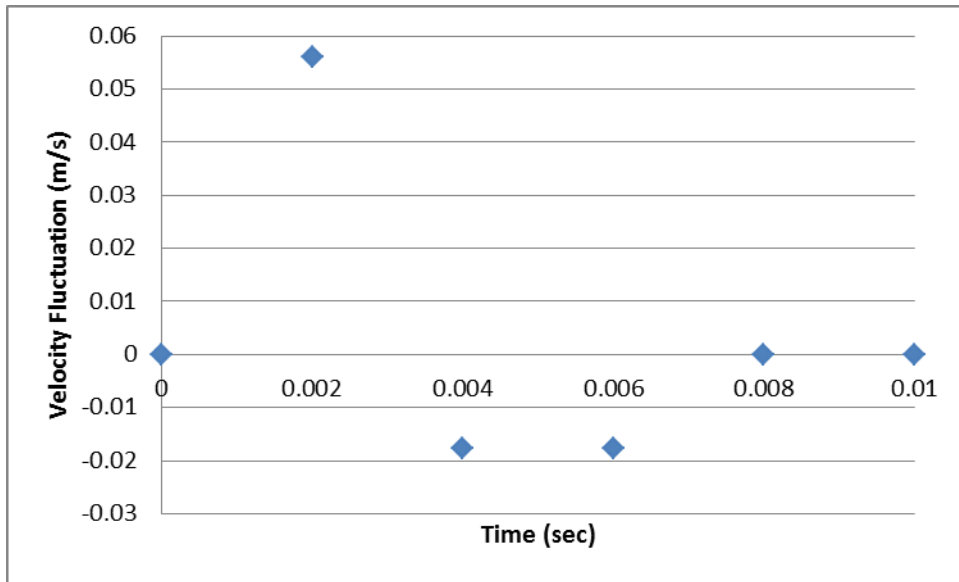
Figure 58: The velocity fluctuation of the projectile with time for the ninth shot.

The velocity results for the projectile fired at 175 volts, Figure 58, show a similar trend to the previous shots. The flight of the projectile begins with a period of increasing velocity fluctuation until a peak of 0.05605 m/s was reached 0.002 seconds into its flight. The peak in velocity is followed by a period of decreasing velocity that bottoms out at a decrease in velocity fluctuation of -0.01759 m/s which was achieved 0.004 seconds into its flight and maintained until 0.006 seconds into its flight. The projectile then returns to the original velocity it achieved in the barrel of the gun. The projectile then "vanishes" from the camera's velocity tracker causing the velocity result at 0.01 seconds into flight to be invalid. The average velocity fluctuation that the projectile achieved was 0.00522 m/s.
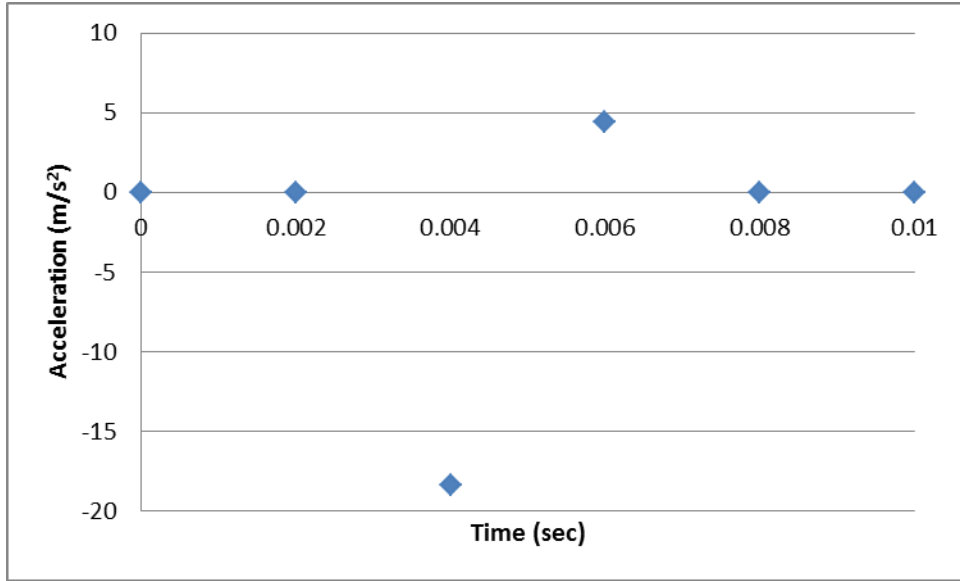
Figure 59: The acceleration of the projectile with time for the ninth shot.

The acceleration results for the projectile shot at 175 volts, Figure 59, once again do not exactly match up with the velocity results. This is due to the fact that the projectile "vanished" from the camera's acceleration tracker for the first 0.002 seconds of its recorded flight. This is followed is a period of deceleration that bottoms out at 0.004 seconds with a deceleration of -18.41 m/s^2 which matches with the velocity results. A period of acceleration occurs after this, which eventually peaks at 4.398 m/s^2 at the 0.006 second mark. The projectile then "vanishes" from the camera's acceleration sensors again for the rest of its recorded flight. The average acceleration achieved by this projectile was -7.00559 m/s^2.

4.11 Combined Results

The results of each shot have been combined graphically in order to provide a visual comparison between the different shots. The shots have been organized into two different categories: the shots that flew in a straight path and the shots that turned in mid-air. The test shot

is not included in the combined results due to the estimated voltage of that shot. The combined

results will be presented with the straight shot results appearing first followed by the shots that
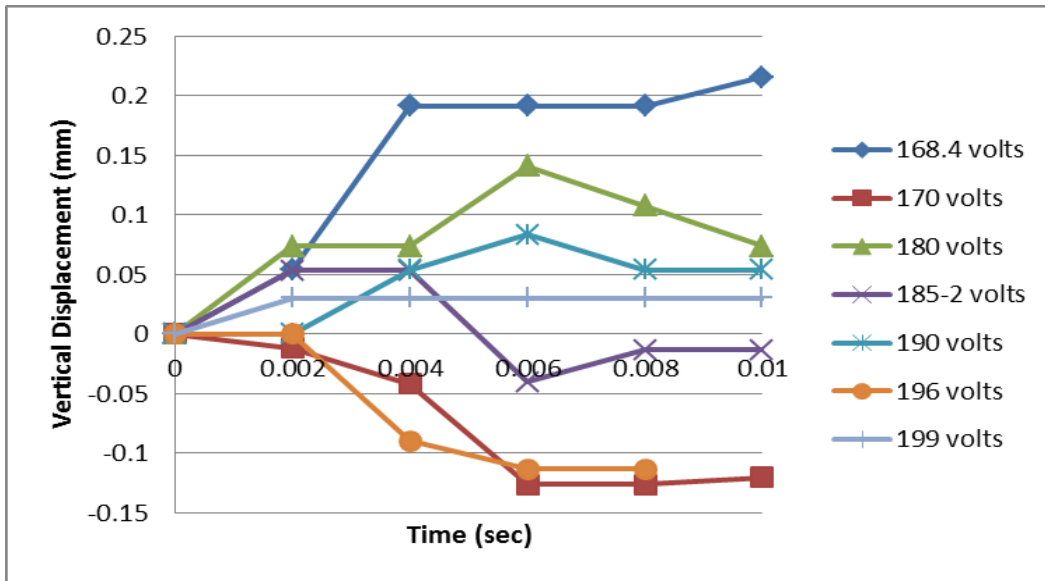
turned in mid-air.

Figure 60: Loss of altitude of the projectile with time for the straight shots.

The combined vertical displacement results for the shots that flew straight are shown in

Figure 60. The projectile shot at 168.4 volts experienced the greatest amount of positive altitude

change. The projectile that experienced the greatest amount of negative altitude change was the

shot at 170 volts. The projectile shot at 199 volts experiences the least amount of change in

altitude; its only change was the result of it tilting, with the remainder of its flight staying at a

steady altitude. This would seem to suggest that a shot at a higher voltage would enable a

straighter flight path for the projectile. The projectile fired at 196 volts does not agree with this

indication though although this could be the result of a change in air flow in the room. The

projectiles fired at 190 volts and 185 volts also seem to confirm this theory that a higher voltage

provides a straighter shot, since both level out during their recorded flight. This result plays less of a factor when the projectile is placed in a reed though, since the reed would maintain a straight flight path. A straighter shot would place less wear on the projectile and reed though, since its flight path would not have to be corrected as much.
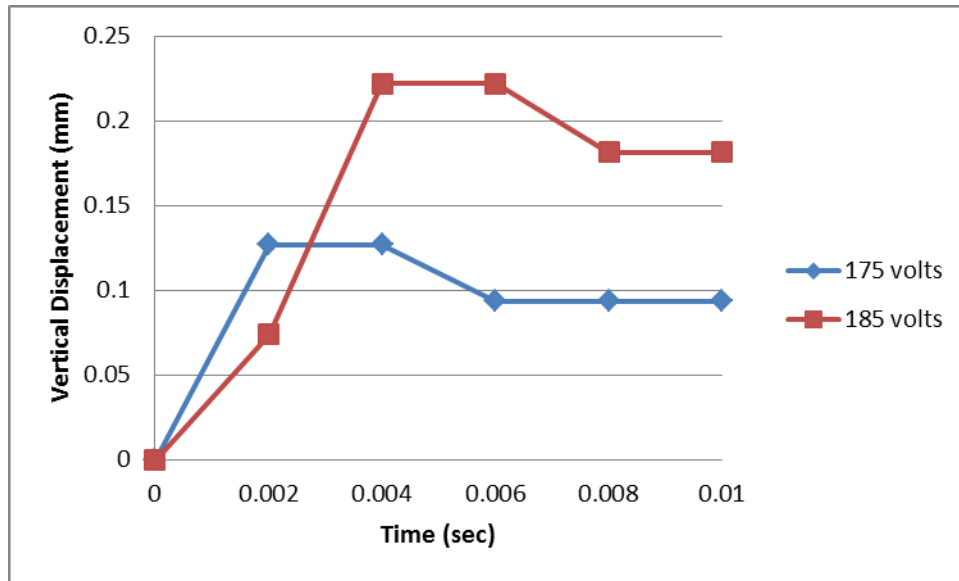

Figure 61: Loss of altitude of the projectile with time for the shots that rotated 90 degrees in mid-air.

The combined results for the vertical displacement of the shots that rotated 90 degrees in mid-air are shown in Figure 61. Both of these shots show almost identical behavior though at differing magnitudes. The projectile fired at 185 volts experiences a greater degree of altitude change than the projectile fired at 175 volts. Both projectiles' altitude eventually level off as they reach the end of their recorded flight. This suggests that a projectile fired at either of these voltages that does not rotate in mid-air would be able to travel through the reed with minimal problems. Firing either of these projectiles in a reed would actually eliminate the chance of the mid-air rotation, since the reed would guide the projectile's flight.
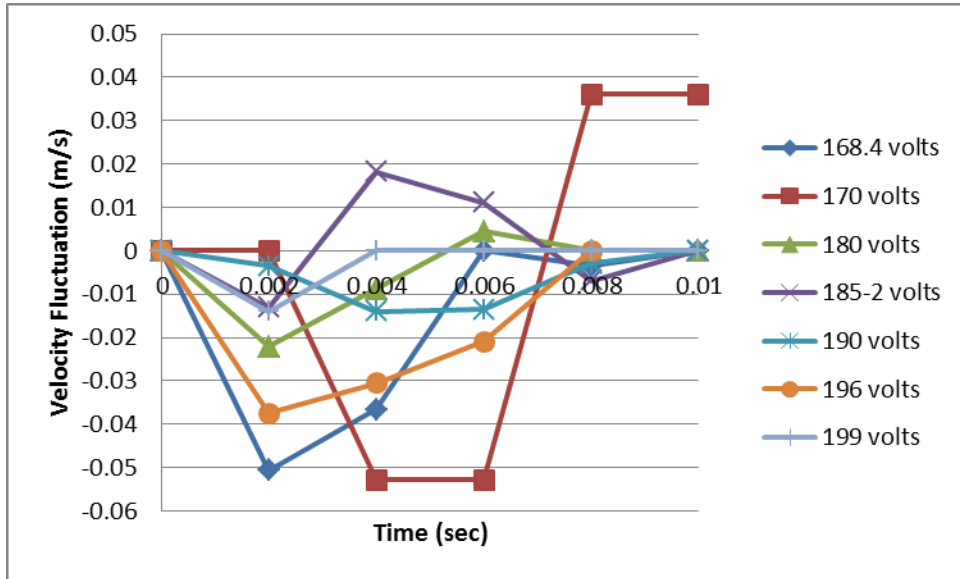
Figure 62: The velocity fluctuation of the projectile with time for the straight shots.

The combined velocity results for the projectiles that flew straight, Figure 62, similar velocity behavior with the projectile first losing speed then gaining speed. The projectile fired at 170 volts shows the greatest degree of fluctuation in velocity having both the most velocity gain and the highest velocity loss. The projectile fired at 199 volts shows the least amount of fluctuation in velocity though it spends the majority of its properly recorded flight below the velocity it achieved in the barrel of the gun.
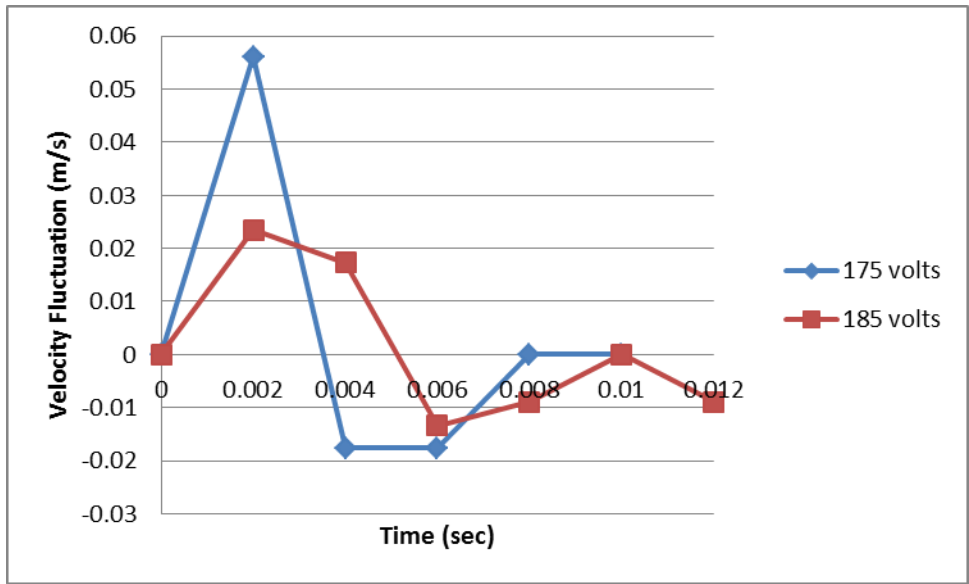
Figure 63: The velocity fluctuation of the projectile with time for the shots that rotated 90 degrees in mid-air.

The combined velocity results for the projectiles that rotated 90 degrees in mid-air, Figure 63, show similar results but at different magnitudes. The projectile fired at 175 volts experiences a greater degree of velocity fluctuation than the shot fired at 185 volts. This includes both a higher peak in increasing velocity and a higher peak in decreasing velocity. The results for the projectiles that rotated in mid-air suggest that, of the two, the projectile fired at 185 volts experiences the least amount of velocity fluctuation.
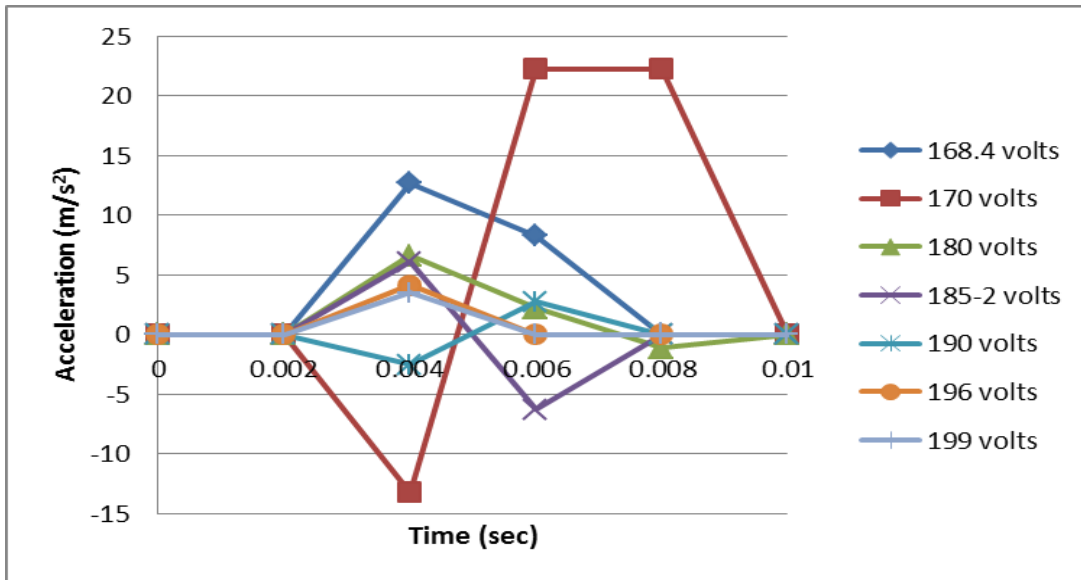
Figure 64: The acceleration of the projectile with time for the straight shots.

The combined acceleration results for the projectiles that flew straight, Figure 64, shows that the projectile fired at 170 volts experiences the greatest variance in acceleration of any of the projectiles. While the shot at 170 volts achieved the highest acceleration, which is desirable in weaving applications, it also achieved the highest deceleration which is not desirable. This makes the power level undesirable for firing through a reed. The projectile fired at 199 volts experienced the least amount of acceleration variance. It should be noted that a majority of the acceleration results are affected by the "vanishing" of the projectile. This is due to the method of tracking the projectiles, which requires the projectile to be manually retargeted once the camera lost track of it. This may affect the camera's ability to calculate the acceleration of the projectile. Why this does not affect the velocity results as often is unknown. It should be noted that there should only be periods of deceleration during the flight of a projectile. The changes in acceleration experienced by the projectiles are the result of the velocity fluctuations they

experienced. This results in both accelerations and decelerations during the flight of the projectile. It should be noted that the changes in acceleration after the coil barrel are negligible.
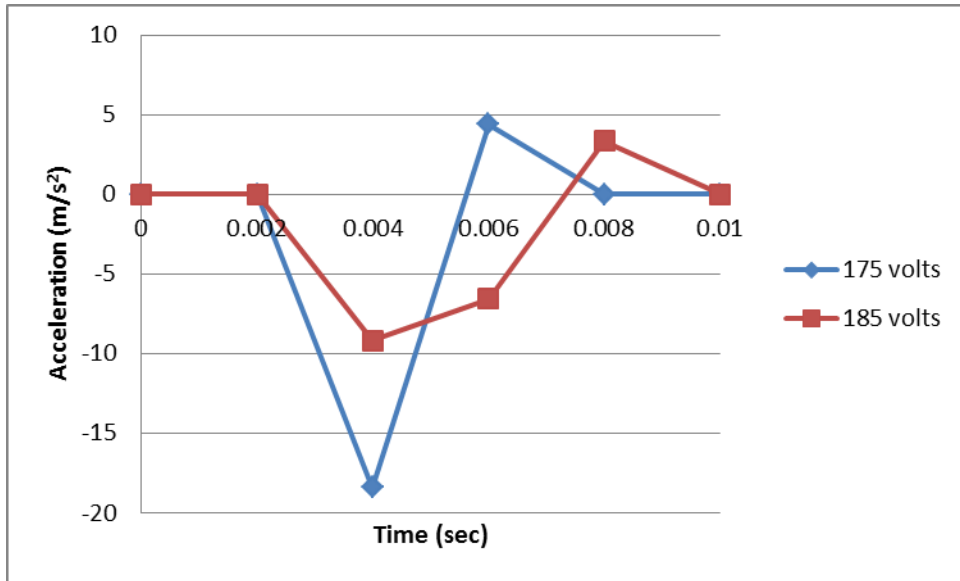

Figure 65: The acceleration of the projectile with time for the shots that rotated 90 degrees in mid-air.

The combined acceleration results for the projectiles that rotated 90 degrees in mid-air, Figure 65, are similar to each other with varying magnitudes of change. The projectile fired at 175 volts experiences greater acceleration and deceleration than the projectile fired at 185 volts. This corresponds to the velocity results in which the projectile fired at 175 volts achieved both higher and lower speeds than the projectile fired at 185 volts. The shot fired at 185 volts again experiences a lesser degree of variance.
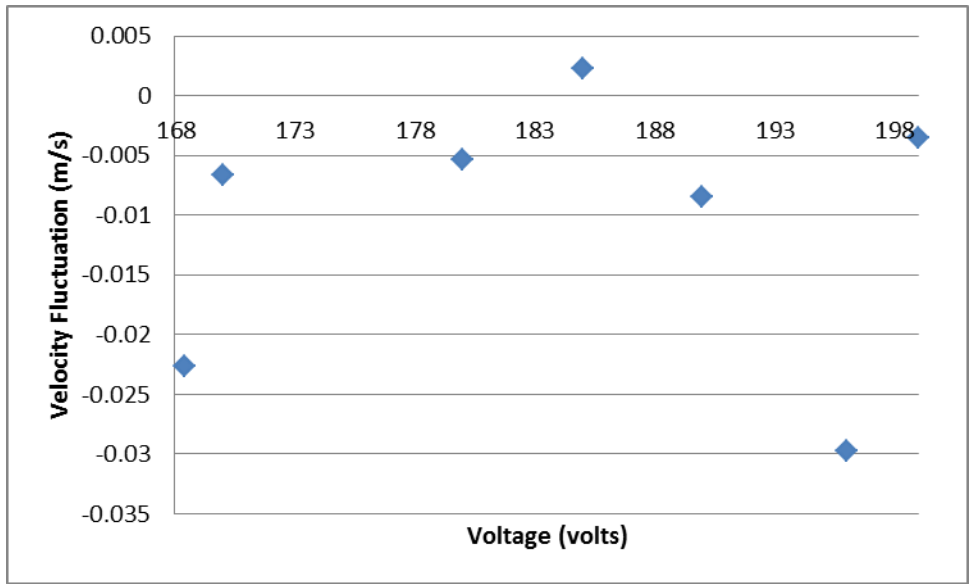
Figure 66: The velocity fluctuation of the projectile as the voltage of the capacitor increases for the straight shots.

Figure 66 shows how the voltage the projectile is fired at affects the average velocity of the projectile. The projectile fired at 185 volts obtained the highest recorded average increase in velocity fluctuation with a velocity of 0.002283 m/s. The projectile fired at 196 volts obtained the highest recorded average decrease in velocity fluctuation of -0.0297 m/s. The results seem to indicate that as the projectiles are launched at greater voltages they experience a lesser degree of velocity fluctuation. This holds true until after the 185 volt shot at which point the average degree of velocity fluctuation increases with increasing power until the shot at 199 volts at which point it began to maintain a lesser degree of velocity fluctuation again.
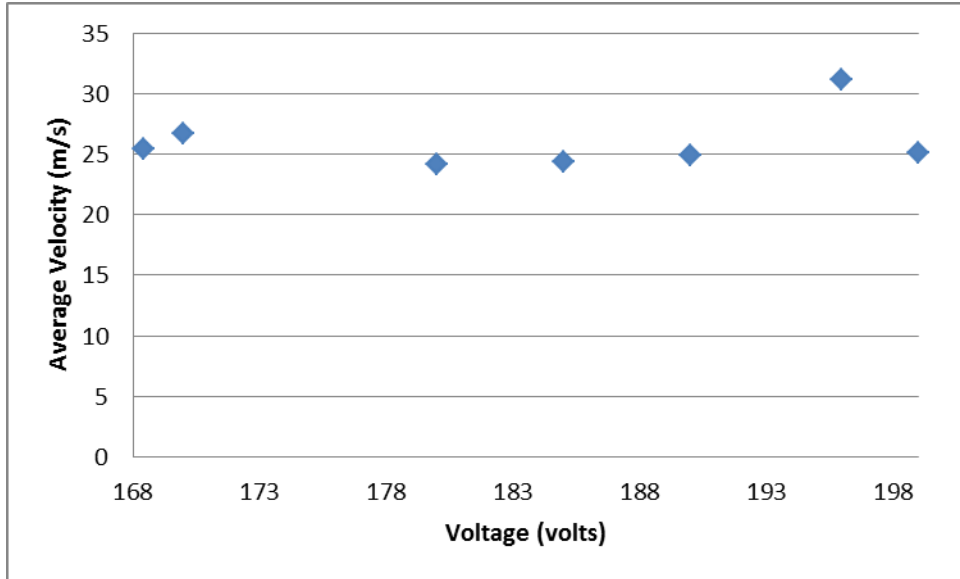
Figure 67: The average velocity of the projectile as the voltage of the capacitor increases for the straight shots.

Figure 67 shows that the lowest average velocity 24.13 m/s was achieved by the projectile fired at 180 volts. Conversely, the highest average velocity was achieved by the projectile fired at 196 volts and was 31.12 m/s. This translates into a filling insertion rate of 1867 meters per minute. Air-jet weaving machines are capable of reaching an average insertion rate of 2400 meters per minute (1). This means that none of the recorded shot power levels are capable of reaching the insertion rate desired under current conditions.
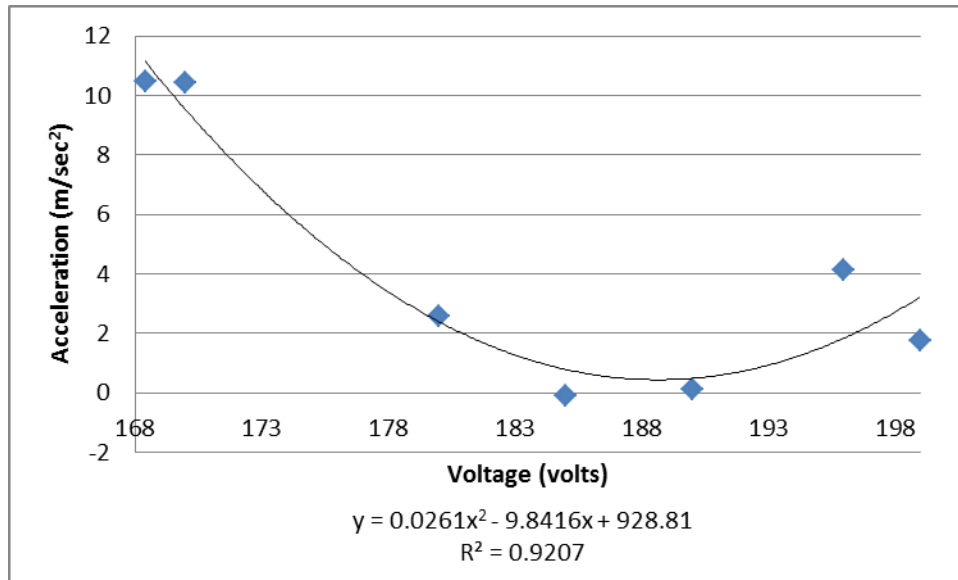
Figure 68: The acceleration of the projectile as the voltage of the capacitor increases for the straight shots.

Figure 68 shows that the voltage the projectile is fired at affects the average acceleration of the projectile. The projectile fired at 168.4 volts obtained the greatest amount of average acceleration which was 10.46 m/s^2. The projectile fired at 185 volts obtained the lowest average acceleration which was -0.09248 m/s^2. The overall results indicate that the lower power levels experience greater acceleration than the higher voltages. This does appear to change after 185 volts though since the shots at both 190 volts and 196 volts have higher acceleration than the previous power levels. The trend appears to re-emerge after 196 volts. This is likely the result of the fact that the lower voltage shots experience a greater degree of velocity fluctuation than the projectiles fired at higher voltages with the exception of the projectile fired at 196 volts.
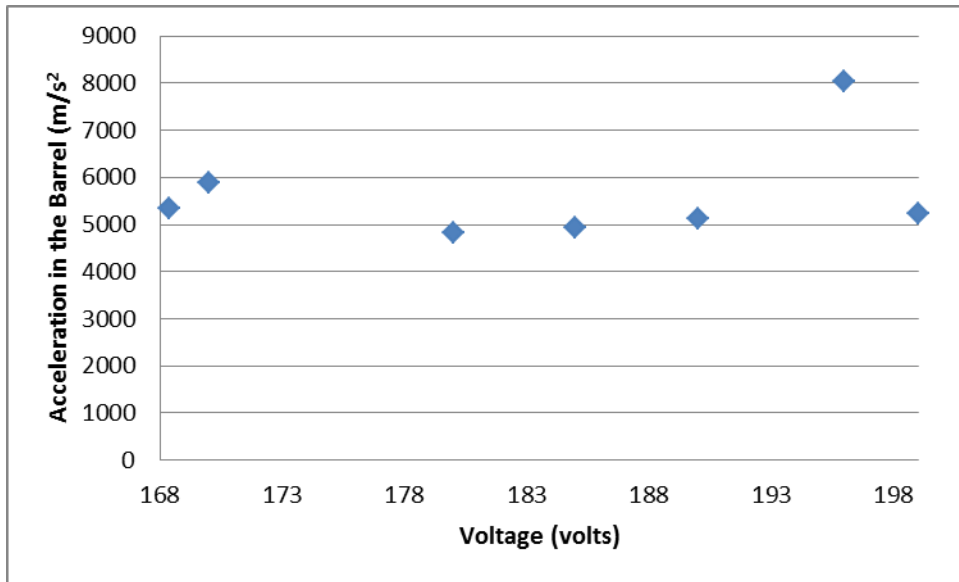
Figure 69: The acceleration in the barrel of the coil gun as the voltage increases for the straight shots.

Figure 69 shows that the lowest acceleration achieved in the barrel of the coil gun was 4826 m/s^2. This acceleration was achieved by the projectile fired at 180 volts which corresponds to the lowest average velocity of the straight shots. Conversely, the projectile fired at 196 volts achieved the greatest acceleration within the barrel of the coil gun which corresponds to the highest average velocity of the straight shots. The acceleration it achieved was 8026.97 m/s^2.

Chapter 5

Conclusions and Recommendations

5.1 Conclusions

The results of this research indicate that the proposed filling insertion system using electromagnetic force to launch the projectile is capable of being used. The projectiles achieved flight with a minimal expenditure of energy. This is important because one of the goals of this new insertion method was to achieve flight with minimum energy usage. The coil gun also launched the projectiles without producing any audible sound. This meets another objective of the new filling insertion method which was to reduce the amount of noise pollution that a typical weaving machine produces. The coil gun did not achieve the insertion speed of current air-jet weaving machines at any of the voltages that the projectiles were fired at. The research was successful in proving the new filling concept may be feasible.

5.2 Future Work

Recommendations for future work on this projectile include determining what voltage the coil gun has to be fired at to achieve the filling insertion that air-jet weaving machines are capable of, determining the flight distance of the projectile, incorporating a reed into the design of the coil gun to simulate the effect of firing the projectile through a reed, and building a larger version of the coil gun to better achieve the project objectives. Finding the proper voltage needed to reach the average filling insertion speed of an air-jet weaving machine is important in order to achieve the original objective of this new insertion system which is to insert yarns faster than any

current filling method. Once the proper insertion speed is reached, the next important step in the future is to determine the maximum flight distance of the projectile at the voltage that gives the higher insertion speed. This will determine the width of fabric that can be produced. A device should be constructed in order to demonstrate the effect the reed will have on the projectile. A solid plastic tube can serve as the reed to simulate the effect of the reed on the projectile. The future work should be developing a larger version of the coil gun. This larger coil gun should make achieving the goals of the project easier and should provide an accurate simulation of how the coil gun that will be incorporated into the weaving machine will use energy resources.

References

1. Adanur, Sabit, Ph.D. Handbook of Weaving. Lancaster, Pennsylvania: CRC, 2002. 2-4, 169-174, 175-219, 219-223, 227-259, 263-290. Print.

2. Adanur, Sabit, Ph.D. Wellington Sears Handbook of Industrial Textiles. Lancaster, Pennsylvania U.S.A.: Technomic Publihing, 1995. 111-120. Print

3. ball point pen. N.d. Photograph. Photo DictionaryWeb. 22 Mar 2012. <http://photo-dictionary.com/phrase/7936/ball-point-pen.html>.

4. "Electrical Tape." Wikipedia, the free encyclopedia. Wikimedia Foundation, Inc., 29 Feb 2012. Web. 6 Mar 2012. <http://en.wikipedia.org/wiki/Electrical_tape>.

5. Fuji Flash Unit 1. N.d. Schematic. Repair FAQWeb. 13 Mar 2012. <http://www.repairfaq.org/sam/fflash1.gif>.

6. Hansen, Barry. Barry's Coilgun Designs. Barry Hansen, 19 Jan 2012. Web. 19 May 2011. <http://www.coilgun.info/about/home.htm>.

7. Hausey, Sheri. "More Photos." Sheri Hausey. N.p., n.d. Web. 6 Mar 2012. <http://sherihausey.com/more/>.

8. Hm-Innovations. "The 0$ Coil Gun." Instructables: ShareWhat You Make. Instructables, n.d. Web. 8 Sep 2011. <http://www.instructables.com/id/The-0-Coil-Gun/?ALLSTEPS>.

9. Kolm, Henry, Kevin Fine, Fred Williams, and Peter Mongeau. "Overview of Electromagnetic Guns: ELECTROMAGNETIC GUNS, LAUNCHERS and REACTION ENGINES." Magnetic Materials. Barry Hansen, 06 Jun 2008. Web. 19 May 2011. <http://www.coilgun.info/theorymath/electroguns.htm>.

10. Mirjalili, S.A. "Using Electromagnetic Force in Weft Insertion of a Loom." FIBRES & TEXTILES in Eastern Europe. 13.3 (2005): 67-70. Web. 19 Jan. 2011. <http://www.fibtex.lodz.pl/51_19_67.pdf>.

11. Verma, Rohit (269 D.K.1, Scheme No. 74-C Indore 0, Madhya Pradesh, 452 01, IN) WO/2005/098109 <http://www.sumobrain.com/patents/WO2005098109.html>.

12. "Weaving/Weaving Mechanism/Classification of Weaving Machines." Textile Learner. Textile Learner, n.d. Web. 6 Mar 2012. <http://textilelearner.blogspot.com/2011/06/weaving-weaving-mechanism_643.html>.

13. Yamaha. "Five Key Tips to Wonderful Wiring: Doing it Right the First Time is the Only Way to Electrical Success." Outdoor Hub: The Outdoor Information Engine. Outdoor Hub, 12 Jul 2011. Web. 6 Mar 2012. <http://www.outdoorhub.com/how-to/five-key-tips-to-wonderful-wiring-doing-it-right-the-first-time-is-the-only-way-to-electrical-success/>.